A Statistical Stability Analysis of Earth-like Planetary Orbits in Binary Systems

Marco Fatuzzo,[1] Fred C. Adams,[2,3] Richard Gauvin[1] and Eva M. Proszkow[2]

[1] *Physics Department, Xavier University, Cincinnati, OH 45207*

[2] *Michigan Center for Theoretical Physics, University of Michigan Physics Department, Ann Arbor, MI 48109*

[3] *Astronomy Department, University of Michigan, Ann Arbor, MI 48109*

fatuzzo@cerebro.cs.xu.edu, fca@umich.edu

ABSTRACT

This paper explores the stability of an Earth-like planet orbiting a solar-mass star in the presence of a stellar companion using $\sim 400,000$ numerical integrations. Given the chaotic nature of the systems being considered, we perform a statistical analysis of the ensuing dynamics for ~ 500 orbital configurations defined by the following set of orbital parameters: the companion mass M_C; the companion eccentricity e; the companion periastron p; and the planet's inclination angle i relative to the stellar binary plane. Specifically, we generate a large sample of survival times (τ_s) for each orbital configuration through the numerical integration of $N \gg 1$ equivalent experiments (e.g., with the same orbital parameters but randomly selected initial orbital phases). We then construct distributions of survival time using the variable $\mu_s \equiv \log \tau_s$ (where τ_s is in years) for each orbital configuration. The primary objective of this work is twofold. First, we use the mean of the distributions to gain a better understanding of what orbital configurations, while unstable, have sufficiently long survival times to make them interesting to the study of planet habitability. Second, we calculate the width, skew, and kurtosis of each μ_s distribution and look for general features that may aid further understanding and numerical exploration of these chaotic systems. To leading order, most distributions are nearly Gaussian with a width $\sigma \sim 0.5$, although the longest-lived systems display substantial (non-Gaussian) tails. As a result, many independent realizations of these systems must be considered in order to characterize the survival time. The situation is more complicated for orbital configurations with longer mean survival times, owing in part to the increasing importance of resonances.

Subject headings: planetary systems

1. INTRODUCTION

Recent (and ongoing) discoveries of exoplanetary systems (e.g., Butler et al. 1999; Marcy et al. 2001; Fisher et al. 2002; Tinney et al. 2002; McArthur er al. 2004) have shown that Sun-like stars are orbited by planets with a wide variety of orbital configurations. Of course, current planetary searches are biased toward large bodies with short orbital periods, resulting in the discovery of planets with masses ranging from $\sim 0.01-10M_J$ and semi-major axis typically ranging from $\sim 0.04-4$ AU. It is expected that Earth-like planets will also form alongside their Jovian counterparts (e.g., Ruden 1999; Lissauer 1993), even in binary stellar systems (e.g., Whitmire et al. 1998; Quintana et al. 2002; Lissauer et al. 2004).

The discovery of exoplanetary systems has spurred a renewed interest in planetary dynamics, with a significant amount of attention being given to the stability of specific multi-planet systems (e.g., Laughlin & Adams 1999; Süli et al. 2005) and to the stability of (hypothesized) terrestrial planets located within a specific system's habitable zone (e.g., Noble et al. 2002; Asghari et al. 2004; Jones et al. 2005; Haghighipour 2006). In addition, the identification of Jupiter-like planets in orbit around members of multiple star systems (e.g., Eggenberger et al. 2004 and references therein) has also provided an observational basis for studying planetary stability in binary systems (e.g., Harrington 1977; Pendleton & Black 1983; Rabl & Dvorak 1988; Holman & Wiegert 1999; David et al. 2003; Pilat-Lohinger et al. 2003; Musielak et al. 2005; Mudryk & Wu 2006). Of course, one must differentiate between stability within a habitable zone and the more general study of overall system stability, with the former imposing stricter conditions on a planet's allowed orbital motion.

Planetary orbits in binary systems can be found with a wide range of configurations. The two most common orbital classes are P-type orbits, in which the planet's semi-major axis is larger than that of the binary so the planet orbits about both stars, and S-type orbits, in which the planet revolves around one of the stars with a semi-major axis smaller than that of the binary (e.g., Szebehely 1967, Dvorak et al. 1989, Pilat-Lohinger & Dvorak 2002). If the semi-major axis of the planetary orbit is sufficiently large (for P-type orbits) or sufficiently small (for S-type orbits), the orbital motion is stable and well-ordered. However, in binary configurations for which the stellar bodies come sufficiently close to the planet, the motion can be chaotic and even unstable. One goal of this paper is to determine the regime of binary parameter space for which S-type planetary orbits are stable. In the regime of parameter space near the border between stability and instability, the orbits tend to be chaotic.

A complete analysis of planetary stability in stellar binaries must reconcile the underlying chaotic nature of the systems being explored. While theoretical conditions can be used to determine whether a planetary system is unstable, it is still possible for such systems to

last for vast spans of time. Numerical work must then be used to delineate the boundaries of "effectively" stable parameter space. However, for a given orbital configuration, the survival time τ_s of an unstable system (defined throughout this work as the number of years it takes for the planet to either be ejected or collide with either star) varies widely depending on the choices of initial orbital phases. Because the systems are chaotic, this variation is not smooth, i.e., small differences in the starting phase angles can lead to large differences in the resulting survival times. As a result, the survival time for any set of binary properties can only be fully characterized in terms of a distribution of output measures. Further, as shown herein, the distribution of survival times has a substantial width. Even though the systems are chaotic in the regime of interest, and hence display a wide distribution of survival times for effectively equivalent starting conditions, we stress that the distributions themselves are well-defined. As a result, the answer to the question – How long does a planet survive in any given binary system? – is a full distribution. One goal of this work is to find such distributions for binary systems with intermediate semimajor axes $a \approx 1 - 50$ AU.

A statistical analysis of the stability of an Earth-like planet orbiting a one solar-mass star in the presence of an outer-lying companion was recently performed by David et al. (2003; hereafter D03), leading to an estimate of the fraction $\mathcal{F}_b$ of binary star systems that allow Earth-like planets to remain in the system over a time scale of 4.6 Gyr. Specifically, D03 found that $\mathcal{F}_b \approx 0.5$ by calculating the survival time of an Earth-like planet (with an initial circular orbit of R = 1 AU) for a range of companion masses $M_C = 0.001 - 0.5 M_\odot$, initial eccentricities e, and semi-major axis a. For the parameter space explored by D03, the planet's survival time (for a specified companion mass) depends most sensitively on the companion's initial periastron distance $p = a(1 - e)$, but spans over two decades when sampled over a range of semi-major axis values (with e then set to give the desired value of p). Nevertheless, the mean value of log τ_s exhibits a clear exponential dependence on the periastron. It is important to note that the range of survival times versus periastron presented in D03 results from both the chaotic nature of the three body problem and the sampling over different (a, e) pairs for a given periastron value (see §5.2 for a more complete discussion).

This paper extends previous work on the stability of an Earth-like planet orbiting a Sun-like star in the presence of a stellar companion. Although much of the previous work focused on coplanar systems (e.g., D03), this work explores the full range of inclination angles. Specifically, we explore ~ 500 different orbital configurations (defined through the choice of the companion mass M_C, eccentricity e, and periastron p, and the planet's inclination angle i relative to the stellar orbital plane), and we broadly sample the orbital parameter space inhabited by most observed binary systems. Our main body of work explores 376 different orbital configurations organized in four series (1 – 4). An additional 136 orbital configurations

with low inclinations, organized in three series (5 – 7), are performed to further explore some of the detailed structure exhibited by the output measures of the first four series. We generate a large sample of survival times (τ_s) for each orbital configuration through the numerical integration of $N \gg 1$ equivalent experiments (with the same basic orbital parameters but randomly selected initial orbital phases), performing a total of $\sim 390,000$ separate orbital simulations; this sample of orbital simulations is thus an order of magnitude larger than our previous study (D03). This broad survey of parameter space provides a cleaner delineation of the orbital configurations that (while potentially unstable) have sufficiently long survival times to be interesting for planetary habitability (as noted above, however, stability within a planet's habitable zone imposes additional constraints on the planet's orbital motion).

Another focus of this new work is the characterization of the distributions of survival times. As discussed earlier, the regime of parameter space near the stability/instability border is chaotic and the results must be described statistically. Performing multiple realizations for each orbital configuration is a necessity. This paper constructs distributions of survival times — using the variable $\mu_s \equiv \log \tau_s$, with τ_s defined in years — for each orbital configuration under consideration. The resulting distributions are then characterized by their mean, width, skew and kurtosis. We also calculate the fraction of runs that lead to the planet's ejection from the system (and the fraction accreted by one of the stars). With the construction of these distributions, we can study how they vary over the regime of binary parameter space; these distributions also provide important guidance for future work (e.g., the width of the distribution determines how many independent realizations of the numerical problem are necessary to achieve a desired accuracy in estimating the mean value).

The paper is outlined as follows: We discuss the numerical method used in our work in §2. We present the results of our numerical work for series 1 – 4 in §3, and characterize the resulting distributions for these series in §4. We present the results of series 5 – 7 in §5, and use the results of these runs to explore certain aspects of the rich structure exhibited by these three body-systems. Specifically, we: 1) consider the effect of integer ratios of initial planet/companion orbital periods – a necessary but not sufficient condition for resonance (see, e.g., Murray & Dermott 2000); 2) explore more fully the dependence of ejection time on eccentricity and on periastron; 3) characterize the fraction of ejection events; and 4) consider the stability exhibited by high inclination, low eccentricity orbits. We present our conclusions in §6.

2. NUMERICAL SCHEME

We present here the numerical method by which we calculate the survival time of an Earth-like planet orbiting a Sun-like star in the presence of a stellar outer companion. Through long term dynamical interactions with the outer companion, the orbital elements of the Earth-like planet evolve, generally in chaotic fashion, until the planet is either ejected from the system or collides with one of the two stars. In order to explore this stability issue on intermediate time scales, Newton's equations of motion are integrated directly using a Bulirsh-Stoer (B-S) scheme (Press et al. 1992). Although direct integration is computationally more expensive (e.g., compared to symplectic integration), it is accurate and explicit. For the systems at hand, our B-S scheme incurs errors in relative accuracy of order 1 part in 10^{11} per total time step, where each time step in the three-body problem is variable, but has a typical value of about 10 days. The accumulated error for a given integration is characterized through the ratio of $\Delta E/E$, where E is the initial system energy (which should be conserved) and ΔE is the difference between this value and the final energy of the numerically integrated system.[1] Since the ratio of the Sun-planet to Sun-companion orbital energy is $\sim (M_p/M_C)(a_C/a_p) \sim 10^{-5}$ for the systems that yield the longest survival times in our study (where a_p is the Earth's semi-major axis), we check *a posteriori* that $\Delta E/E$ remains less than $\sim 10^{-6}$ to ensure that accumulated errors do not affect our results.

The planet's initial orbit is always set to be circular ($e_p = 0$) with radius $R = a_p = 1$ AU. The companion mass M_C, eccentricity e, and periastron p, as well as the planet's initial inclination angle i (relative to the stellar binary plane) are then specified for each run, and the system is integrated forward in time. For the sake of definiteness, and in order to cover a large range of parameter space, we use an upper limit integration time of $\tau_{run} = 10^8$ years for the runs presented in §3 (series 1 – 4), and $\tau_{run} = 10^9$ years for the runs presented in §5 (series 5 – 7). Our experiments therefore give us either a time scale for survival or a lower limit of τ_{run} on the possible survival time. The planet is considered to be ejected if any of the following conditions are met: The energy of the planet becomes positive; the eccentricity of the planet exceeds unity; or the semi-major axis of the planet exceeds a maximum value (taken here to be 100 AU). The planet is considered to collide with the solar mass star if the periastron of the planet becomes smaller than the stellar radius (assumed to be 1 $R_\odot$) so the planet is accreted, and to collide with the companion if its orbit crosses within one radius of the companion's center-of-mass position (although for the orbital configurations considered here, the latter result is effectively ruled out). The survival time for a given

[1]The error accumulation involves a random walk process so that high accuracy can (usually) be maintained even when the product of the error per time step and the number of time steps exceeds unity.

orbital configuration is explored statistically by sampling over N equivalent realizations set through the random assignment of the initial orbital phase angles, where $N = 10^3$ for series 1 – 4 (presented in §3) and $N = 10^2$ for series 5 – 7 (presented in §5).

3. RESULTS OF PARAMETER SPACE SURVEY

This section presents the results of 376,000 numerical experiments with orbital parameters organized into four series with the following $[M_C, e]$ values: (1) $[0.1M_\odot, 0.5]$; (2) $[0.5M_\odot, 0.5]$; (3) $[0.5M_\odot, 0.75]$; and (4) $[0.5M_\odot, 0.25]$. Values for the companion periastron and the planet's inclination angle relative to the Sun-companion orbital plane range from $p = 2 - 6$ AU and $i = 0^o - 90^o$, respectively, for each series.[2] A total of $N = 10^3$ equivalent realizations (with initial phase angles sampled randomly) were performed for each of the 376 different orbital configurations explored (defined by the parameter space four-vector $[M_C, e, p, i]$).

For the chaotic systems being explored herein, different choices of the initial phase angles can lead to widely different dynamical behavior, and hence the values of survival time τ_s can differ by orders of magnitude for effectively equivalent starting states. The survival time for a given orbital configuration is best characterized in terms of a distribution in $\mu_s \equiv \log \tau_s$ (where the survival time is expressed in years). Each orbital configuration is therefore characterized by the mean or expectation value $\langle \mu_s \rangle$, the width

$$\sigma = \left[\frac{\Sigma(\mu_s - \langle \mu_s \rangle)^2}{N} \right]^{1/2} , \tag{1}$$

the skew

$$\mathrm{sk} = \left[\frac{\Sigma(\mu_s - \langle \mu_s \rangle)^3}{N\sigma^3} \right] , \tag{2}$$

and the kurtosis

$$\mathrm{ku} = \left[\frac{\Sigma(\mu_s - \langle \mu_s \rangle)^4}{N\sigma^4} \right] - 3 , \tag{3}$$

of its corresponding distribution. A secondary output measure also explored here is the fraction f_e of ejection events, defined as the number of runs that result in the planet being ejected from the system divided by the total number of ejection/accretion events (see §5 for further discussion).

[2]Although high-inclination configurations have been included for completeness, observations suggest that planetary systems are likely to form in binaries with relatively small ($i \lesssim 20^o$) inclination angles. For example, disks in binary systems are close to coplanar (e.g., Mathieu et al. 1991).

The calculated values of $\langle \mu_s \rangle$ are plotted versus inclination angle i for several periastron tracks in Figure 1, with series 1 – 4 separated into panels (a) – (d). For all cases, a clear transition between longer and shorter lived systems occurs at $i \sim 40^o$, in agreement with results of previous studies (e.g., Harrington 1977; Pendleton & Black 1983; Innanen et al. 1997; Haghighipour 2006). Additionally, a clear region of stability is found at $i \approx 60^o$ for series 4. Note that Kozai resonances occur for large inclination angles (see §5 for further analysis and discussion).

Clear trends are exhibited by our results. As expected, survival time depends strongly on the companion mass and periastron, and somewhat weakly on inclination angle for $i \lesssim 40^o$. In addition, panels (b) – (d) in Figure 1 corresponding to series 2 – 4 ($M_C = 0.5 M_\odot$; $e = 0.5, 0.75$ and 0.25) indicate that while survival times increase with eccentricity for periastron values below $p \sim 3$ AU (as one would naively expect given the longer orbital period of the companion orbits), the opposite trend is suggested for periastron values greater than 3 AU. The dependence on survival time on eccentricity will be further explored in §5. The robust structure of orbital systems (being chaotic in nature) is also clearly illustrated by the interweaving of the $p = 2.5$ AU and $p = 3$ AU tracks in panel (a) of Figure 1. Naively, one expects the survival time to increase with increasing periastron, and this general trend is clearly seen in all four panels of Figure 1. The enigmatic behavior of the $p = 3$ AU case in series 1 thus suggests some type of resonance behavior. Indeed, this set of orbital parameters corresponds to an initial companion orbital period exactly 14 times larger than the planet's, a necessary but not sufficient condition for resonance to occur (e.g., Murray & Dermott 2000). We more fully explore the structure associated with integer ratios of initial orbital periods in §5.

One goal of this work is to determine what region of orbital parameter space may be of interest to the study of planet habitability. It is well known that many planetary systems, while Hill unstable, can survive long enough to make them effectively stable on time scales comparable to the age of the Universe (but as previously noted, the stability criteria explored in this paper is not the same as stability within a habitable zone). Extrapolating the results of our work provides an estimate of the minimum companion periastron values p_{min} required for an Earth-like planet orbiting a Sun-like star to remain stable in a stellar binary system for ~ 5 Gyrs (a time scale comparable to the current age of the Solar System). Doing so in the low inclination angle regime leads to an estimate of $p_{min} \sim 4$ AU for a companion mass of $M_C = 0.1 M_\odot$ (see also Figure 8 and §5), and $p_{min} \sim 6$ AU for $M_C = 0.5 M_\odot$ (see also Figure 13 and §5). These results are in good agreement with the conservative estimate of $p \sim 6 - 7$ AU for a 4.6 Gyr survival time obtained by D03.

4. WIDTHS OF THE DISTRIBUTIONS

The characterization of the survival times through the output measure $\mu_s \equiv \log \tau_s$ was motivated by the large dynamic range of survival times exhibited by different realizations of the same orbital configuration. Although the use of a logarithmic time unit is arbitrary, it appears to be robust for the cases explored in series 1 – 4. Specifically, the distributions of μ_s for most of the orbital configurations presented in §3 are nearly Gaussian to leading order, i.e., τ_s is log-normally distributed; further, the distributions have roughly the same widths $\sigma \sim 0.5$. To further illustrate this point, panels (a) – (c) of Figure 2 show the distributions of μ_s values obtained for orbital configurations with $M_C = 0.1 M_\odot$, $p = 2.5$ AU, $e = 0.50$ and $i = 0^o$, 25^o, and 50^o, along with corresponding Gaussian distributions (solid line) with the same computed mean, width, and normalization.[3]

Interestingly, distributions in our survey with $\sigma \gtrsim 0.7$ also appear to have Gaussian peaks with widths ~ 0.5, where the presence of tails leads to the higher computed values of the total widths. As an example, the distribution for the orbital configuration $M_C = 0.5 M_\odot$, $p = 3.5$ AU, $e = 0.50$ and $i = 35^o$ is shown in Figure 2, panel (d). Again, the solid line represents a Gaussian profile with the same width, mean and normalization as the computed distribution. Clearly, the presence of a tail above the peak makes the overall profile wider and non-Gaussian.

One of the most important aspects of this work is the characterization of the μ_s distribution widths. These values quantify the degree of chaos in these three-body systems and allow one to determine the precision of the mean value $\langle \mu_s \rangle$ calculated from N equivalent numerical experiments. For example, if the parent distribution is nearly Gaussian, then the mean value calculated from N equivalent numerical experiments has a 68%, 95% and 99% probability of being within 1, 2, and 3 $\sigma/\sqrt{N}$, respectively, of the true mean.

The dependence of the distribution width on inclination angle and on mean survival time (characterized by $\langle \mu_s \rangle$) for the distributions of the 376 orbital configurations in series 1 – 4 is illustrated by the scatter plots presented in panels (a) and (b) of Figure 3. The solid line in panel (a) connects the mean widths calculated at each inclination angle, determined by combining all of the results from orbital configurations with the same inclination angle (but offset by the mean so as to center each distribution about zero) to form a single distribution,

[3]The degree to which a given distribution is non-Gaussian is measured by its skew and kurtosis. The skew reflects how symmetric about the mean value a distribution is, with "right-heavy" distributions having positive skews. The kurtosis reflects how peaked or flattened a distribution is, with flatter than normal distributions having a positive kurtosis, and pointier than normal distributions having a negative kurtosis (e.g., Press et al. 1992).

and then calculating the ensuing width as per equation (1). Most of the distributions for the orbital configurations considered in this section have widths in the range $\sigma \sim 0.2 - 0.6$. In addition, the distribution width has only a weak dependence on inclination angle, and no clear trend that differentiates the four series from each other. The distribution width also seems independent of the mean survival time for orbital configurations with $\langle \mu_s \rangle \lesssim 4$, although wider distributions appear increasingly likely when $\langle \mu_s \rangle \gtrsim 4$. This result is further explored in §5.

A proper interpretation of the meaning of a width calculated from a sample distribution requires an underlying assumption about the parent distribution from which the sample was drawn. To assess the meaning of the values of σ calculated for the orbital configurations in series 1 – 4, we need to gauge whether a Gaussian approximation for the calculated μ_s distributions is warranted. Toward this end, we present scatter plots of skew and kurtosis versus width in panels (c) and (d) of Figure 3 for the distributions of the 376 orbital configurations of series 1 – 4. The dotted lines in these figures represent the three-sigma values (for the parameter relevant to the given panel) calculated through random sampling (with $N = 10^3$) of a Gaussian parent distribution. For example, the skew of a sample distribution built-up by randomly sampling a Gaussian parent distribution 10^3 times would have a 99% probability of falling within the dotted lines of Figure 3, panel (c). Clearly, the overwhelming number of orbital configurations lead to distributions with positive skew and kurtosis, with most skew values ranging between 0 and 2, and most kurtosis values ranging from 0 and 5. No obvious trends differentiate series 1 – 4 in this respect. As a point of reference, we note that the distributions shown in Figure 5 (plotted in terms of ln P) have values of skew between 1 and 1.2, and values of kurtosis between 5 and 8. Clearly, while the distributions explored in this section are not perfectly Gaussian, they nevertheless have Gaussian-like peaks, and to first order, can be reasonable well approximated by Gaussian profiles. Furthermore, the departure of the distributions from a Gaussian form occurs through a tail at high values of μ_s.

To gain further insight into the distribution widths expected from this class of systems, we produce histograms of survival times for subsets of the orbital configurations in series 1 – 4, with each survival time normalized about the mean of its own distribution (i.e., all of the distributions are normalized so that their mean is zero, and then combined to form new distributions for specific subsets of the data). Figure 4 shows the resulting histograms for each series, plotted in terms of the natural log of the probability P and normalized values of μ_s. Figure 5 presents the resulting histograms for series 2 – 4 (panel [a]) and for various angle subsets of series 2 – 4 (panels [b] – [d]). The width of each distribution is included in the figures; the skew and kurtosis for each of the histograms range from 1 to 1.6, and from 3 to 8, respectively. In all cases, power exists in the wings, but a clear peak is always observed.

Figure 6 presents probability histograms of σ for all of the distributions within each of the four series (these histograms thus represent the distribution of distribution parameters). The calculated mean width $\langle\sigma\rangle$ and distribution width σ_σ are denoted in each panel. We note that the calculated values of $\langle\sigma\rangle \sim 0.35$ are slightly lower than the mean of the distributions shown in Figures 4 and 5. Similar histograms for all of the distributions in series 2 – 4 as well as the low angle ($i \leq 30^o$) subset are presented in Figure 7.

For the orbital configurations explored in this section, distributions have typical widths in the range $\sigma \sim 0.2 - 0.6$. Taken at face value, a "typical" distribution of μ_s for the most likely orbital configurations found in our galaxy (i.e., $i \lesssim 20^o$) is expected to have a width of $\sigma \sim 0.5$ (see the discussion of §5.3 for further complications). As a result, the value of $\langle\mu_s\rangle$ calculated through a random sampling with a sample size of N would have a 68% probability of being within $\sim 0.05\sqrt{(100/N)}$ of the true value, and a 99 % probability of being within $\sim 0.15\sqrt{(100/N)}$ of the true value, assuming that the parent distribution is nearly Gaussian. This result provides important guidance for future studies on the survival time of planetary systems.

5. STRUCTURE IN THE OUTPUT VARIABLES

The chaotic nature of three-body problems can lead to a rich amount of structure in the output variables that characterize the underlying dynamics. Indeed, a fair amount of structure is evident in the output measures presented in §3. We explore certain aspects of that structure here through three additional series of runs. Specifically, we consider: 1) the structure resulting from integer ratios of the initial companion/planetary orbital periods; 2) the dependence of survival time on periastron and eccentricity; 3) structure in the output measure f_e – the fraction of simulations for a given orbital configuration that lead to the planet's ejection, and 4) the structure at $\sim 60^o$ evident in panel (d) of Figure 1. The numerical experiments presented in this section (series 5 – 7) were integrated to a maximum run time of $\tau_{run} = 10^9$ years. To compensate for this increase, the number of equivalent experiments performed for each orbital configuration was reduced to $N = 10^2$. Based on the results of §4, we still expect good statistical results. The overall goal of this section is to explore further the aforementioned observed structure in the output variables, to provide some insight into the underlying mechanisms, and to relate this work to results of previous studies of orbital dynamics.

5.1. Mean motion orbital resonances

As noted in §3, the mean value of $\mu_s \equiv \log \tau_s$ generally increases with increasing periastron. This result is expected, given that an increase in periastron corresponds to both an increase in distance of closest approach between the planet and companion and an increase in the companion's orbital period P_b (for a constant eccentricity). However, orbital configurations in series 1 with $p = 3.0$ AU and inclination angles $25^o \leq i \leq 60^o$ have μ_s distributions with smaller means than their $p = 2.5$ AU counterparts, and distributions with smaller means than their $p = 2.9$ AU counterparts at all but the largest inclination angles. As noted in §3, this result suggests the presence of a resonance condition at $p = 3.0$ AU, and indeed, the companion and planet's orbital periods are in a ratio of $n_C : n_p = 14 : 1$.

The presence of resonance conditions can play an important role in the dynamics of a planetary system – and certainly do so in our own solar system (see, e.g., Murray & Dermott 2000 for a thorough discussion). While an extensive review of resonances is beyond the scope of this paper, we note that an integer ratio of initial orbital periods of the planet and companion star can have either a stabilizing or destabilizing effect on the system, depending on the initial positions of the two objects. For example, for a $2 : 1$ orbital configuration, if the planet and the companion start at conjunction at the companion's aphelion, their closest approach distance attains its largest possible value. One would therefore expect such an initial condition to lead to an increase in the planet's survival time. In contrast, if the planet and companion start at conjunction at the companion's perihelion, their closest approach distance attains its smallest possible value. This initial condition therefore has a destabilizing effect on the planet's orbital motion. The goal of this section is to explore what effect the presence of mean motion orbital resonance conditions has on the survival time distribution for randomly chosen initial orbital phases, which in turn affects the structure of output variables generated in this type of analysis.

Toward this end, we first consider a series of low inclination runs with $M_C = 0.1 M_\odot$ and $e = 0.5$, for which the ratio of initial orbital periods is either of the form $n_C : 1$ or $n_C : 2$, ranging from $7 : 1$ to $14 : 1$ (series 5). The results of these experiments are presented in Figure 8, which plots the mean value of μ_s for a given orbital configuration as a function of periastron. Values from $n_C : 1$ orbital configurations are represented with solid point-type, and the value of n_C is marked below the corresponding data. Values from $n_C : 2$ orbital configurations are represented with open point-type. As expected, the mean $\langle \mu_s \rangle$ exhibits an overall increase with increasing periastron, but for orbital configurations with $\langle \mu_s \rangle \gtrsim 4$, the survival times for cases with $n_C : 1$ ratios are clearly shorter than those of their $n_C : 2$ counterparts. Interestingly, both cases correspond to necessary (but not sufficient) condition for resonance (e.g., Murray & Dermott 2000). Our results thus indicate that stabilization is

more likely to occur for integer ratios of the form $n_C : 2$ compared to the $n_C : 1$ case. Indeed, of the 4,200 runs performed in series 5 (100 equivalent realizations for each of the 42 orbital configurations explored), 38 of the 42 experiments that remained bound over the $\tau_{run} = 10^9$ yr span had $n_C : 2$ orbital configurations. Further evidence of enhanced stabilization in the $n_C : 2$ cases is provided in Figure 9, which shows the μ_s distributions for the $11 : 1$, $23 : 2$ and $12 : 1$ orbital configurations ($i = 0^o$) from series 5 (we note that the last bin for the 23:2 distribution contains 7 numerical experiments which survived out to the maximum integration time of 10^9 years). While all three distributions show peaks with widths ~ 0.5, the $23 : 2$ distribution (whose orbital configuration has a periastron that falls between those of the 11:1 and 12:1 cases) has its peak centered at a considerably larger value of μ_s than the others, and has a significant, almost flat tail above the peak.

While a full exploration of the effects of mean motion resonances in these three body systems is not computationally feasible, we perform a series of runs (series 6) focusing on the $11 : 1$ to $12 : 1$ region of series 5. The results of these experiments are presented in Figure 10, with the mean value of the μ_s distribution for a given orbital configuration plotted as a function of periastron at $i = 0^o, 10^o$, and 20^o. Figure 10 suggests that a significant amount of structure can be attributed to $n_C : n_p$ type resonances, and that the survival time is longest for larger values of n_p. This latter result is further suggested by the plot of the width of the μ_s distributions as a function of periastron, as shown in Figure 11. Clearly, the distributions with the greatest widths are associated with large n_p type orbits. Nevertheless, Figure 10 suggests that the dominant features present in the $\langle \mu_s \rangle$ - p curve are broad "depressions" which occur around the $n_C : 1$ orbits. Figure 8 further suggests that these "depressions" become more pronounced with increasing periastron (and hence increasing $\langle \mu_s \rangle$). This issue is complicated and could be the subject of a considerably broader investigation.

An important consequence of these results is the implied additional computational cost in numerically determining the survival times for long-lived systems. Specifically, it appears that μ_s distributions can become significantly wider than ~ 0.5 for orbital configurations with longer survival times, e.g., as shown in Figure 12. This result thus presents an added challenge to the numerical exploration of long-lived planetary systems. In addition to the increased computational time required to perform a given numerical experiment, the number of equivalent runs that must be performed to acquire a valid statistical result for each orbital configuration also increases.

5.2. Ejection time versus periastron and eccentricity

Previous work on the dynamical stability of Earth-like planetary orbits in binary systems (e.g., D03) suggests that the most important variables affecting the system's survival time are the companion mass and periastron distance. In the work of D03, two surveys of the $a-e$ plane were performed using two different numerical methods (both B-S and a symplectic integration scheme). Although the survey of parameter space was not as extensive at that of the present paper, the results are in good agreement with those found herein (see below; see also Holman & Weigert 1999). The mean survival time of a planet in a binary system can be described by a function of periastron of the form

$$\tau_s = \tau_{s0} \exp\left[\alpha(p-1)\right] \ , \tag{4}$$

where periastron p is in AU and the values of α and τ_{s0} depend on the companion mass (e.g., see bottom panels of Figures 3 – 6 and Table 1 in D03). For a given periastron value, the survival time has a relatively wide distribution and equation (4) provides a fit to the mean values.

We note that the width of the distribution of survival times (at constant periastron) arises from two sources: (1) The chaotic nature of the system, which leads to an intrinsic width for any unstable orbital configuration, i.e., for given values of (a, e); and (2) The sampling over (a, e) pairs at constant periastron p, which provides an additional systematic width to the distribution. As discussed in §3, the intrinsic width typically has a value $\sigma \sim 0.5$ (for the distribution of $\mu_s = \log \tau_s$), although the tails at long survival times can make the effective total width larger. The range of survival times, for a given periastron, is wider still, where the additional variation is due to the systematic width defined above.

Figure 13 presents an analogous plot of survival time as a function of periastron p for the simulations of this paper. Specifically, we plot the mean values of μ_s versus periastron for our numerical simulations of the low inclination ($i \leq 20^o$) configurations with $M_C = 0.5 M_\odot$ (series 2 – 4). The figure also shows the value of τ_s calculated from equation (4) using the values of $\alpha = 4.7$ and $\tau_{s0} = 0.64$ given in Table 1 of D03 (appropriate for $M_C = 0.5 M_\odot$). The results of this present work are thus in good agreement with those of D03.

We explore more carefully the structure in our output measures arising from different eccentricities by performing a series of runs with $M_C = 0.5 M_\odot$ and $i = 0^o$, sampling over eccentricity for values of p ranging between 2.5 and 4.5 AU (series 7). As with series 5 and 6, $\tau_{run} = 10^9$ yrs and $N = 10^2$. The results of these experiments are presented in Figure 14, which shows the mean of the μ_s distributions versus eccentricity for different periastron values. The shapes of the $\mu_s - e$ curves (for a given periastron value) indicate the presence of competing effects on the stability of the orbital systems being explored. Specifically, for a

given periastron, an increased value of eccentricity leads to a longer orbital time, and hence a longer time between closest approaches. As a result, one expects an increase in survival time with increasing eccentricity – a clear trend in the high e part of the periastron tracks shown in Figure 14. However, lower eccentricity orbits also become more stable in spite of the reduced orbital times. This result points to the importance of the tangential component of the impulse imparted on the planet at closest approach on destabilizing the system. As a result, low eccentricity orbits (for which these tangential components are small) can have very long survival times. Indeed, a comparison between $e = 0.2$ and 0.8 orbits (with all other orbital parameters the same), as shown by the μ_s distributions in Figure 15, illustrates how dramatic this effect can be.

As with the widening of distributions due to the presence of integer ratios of orbital periods, the stabilization of low eccentricity orbits poses a two-fold challenge for the numerical analysis of such systems. An increasing survival time requires longer integration times, and an increasing width of the distribution requires an increase in the number of equivalent experiments that must be performed in order to gain good statistical output measures. On the other hand, binary systems are likely to have large eccentricities. Specifically, the eccentricity distribution for binaries with orbital periods $P_b \geq 1000$ days (e.g., $a_C \geq 2$ AU) has the form $f(e) = 2e$ (Duquennoy & Mayor 1991), so that low eccentricity orbits are considerably less common than their high-eccentricity counterparts.

5.3. Ejection versus accretion events

In this section we consider the presence of structure in the output measure f_e, the fraction of events that are ejected from the system (excluding events that remain bound for the duration of the numerical run-time τ_{run}). In order for ejection to occur, the gravitational energy between the planet and companion at closest approach must exceed the corresponding gravitational energy between planet and Sun. Since the nearest possible approach d between planet and companion is $d \sim p - 2$ AU (when the planet's eccentricity is near unity), we find that ejection is not energetically possible when $p \gtrsim 2 + 2M_C/M_\odot$, or $p = 2.2$ AU for series 1, 5, and 6 and $p = 3$ AU for series 2 – 4 and 7. This result agrees relatively well with the results of our numerical experiments, especially for low inclination angles. Our results also indicate a clear dependence for f_e on inclination angle, as can be seen from Figure 16, which plots f_e versus inclination angle at different periastron values for series 1 – 4. As a general trend, ejection fraction values peak at inclination angles ranging between 30^o and 60^o, but additional structure is seen in the $f_e - i$ curves.

5.4. Kozai resonance

Figure 1, panel (d) shows a clear peak at $\sim 60^o$, a feature that can be attributed to the presence of a Kozai resonance (e.g., Murray & Dermott 2000). This type of resonance exists for low-mass objects in highly inclined orbits perturbed by an larger mass object with an outer, nearly circular orbit (which explains why the feature is not observed at higher companion eccentricities). At a Kozai resonance, the eccentricity and inclination angle of the planet are coupled such that when one is at its maximum value, the other is at its minimum (and vice versa), and the quantity

$$H_K = \left(a_C \left[1 - e^2\right]\right)^{1/2} \cos i \tag{5}$$

remains constant (Kozai 1962).

To confirm the presence of Kozai resonances in the $\sim 60^o$ runs of series 4, we numerically determine both the planet's eccentricity and inclination angle as a function of time for three different test runs, defined by the orbital parameters: Run 1 – $M_C = 0.5 M_\odot$, $p = 4$ AU, $e = 0.75$ and $i = 0^o$; Run 2 – $M_C = 0.5 M_\odot$, $p = 4$ AU, $e = 0.75$ and $i = 60^o$; Run 3 – $M_C = 0.5 M_\odot$, $p = 4$ AU, $e = 0.25$ and $i = 60^o$. The first two runs have orbital configurations that should not lead to the presence of Kozai resonances owing to a small inclination angle and/or a large eccentricity, whereas Run 3 meets the required conditions for Kozai resonances to occur. The results of the three simulations are shown in Figure 17, which plots the eccentricity for the planet as a function of time (over the planet's survival time) in panels (a) – (c), and the eccentricity (solid line) and inclination angle (dotted line) for a short time interval of Run 3 in panel (d). The latter panel shows a clear periodicity in eccentricity and inclination angle as expected during a Kozai resonance. We also plot the value of H_K as a function of time for each run in Figure 18. The value of H_K clearly oscillates between 0.23 and 0.27 for most of the duration of Run 3, indicating that while the system is not perfectly in resonance (since H_K is not exactly constant), it is close to it. In contrast, the values of H_K for Runs 1 and 2 show considerably more variability.

6. CONCLUSION

This paper extends previous work on numerical simulations of Earth-like planets in binary systems. Specifically, the survival time of an Earth-like planet orbiting a Sun-like star in the presence of an outer companion is determined for different orbital configurations, defined by the companion's mass, eccentricity, periastron, and the planet's inclination angle relative to the binary orbital plane. Due to the chaotic nature of the systems being explored, the survival time for each orbital configuration was determined for N equivalent realizations

with randomly selected initial phase angles, allowing for a statistical analysis of the survival time. We used $N = 10^3$ for the bulk of our exploration of parameter space, which focuses on four pairs of companion masses and eccentricities (series 1 – 4), and $N = 10^2$ for three additional series of runs (5 – 7). In all, we performed $\sim 400,000$ numerical integrations and explored ~ 500 different orbital configurations. Our results indicate that the values of survival time obtained for a given orbital configuration are log-normally distributed (to leading order). We therefore use the logarithm of the survival time $\mu_s \equiv \log \tau_s$ (where τ_s is given in years) as our primary output measure.

We plot the dependence of $\langle \mu_s \rangle$ on inclination angle and periastron value for each distribution in series 1 – 4. These results confirm a weak dependence of survival time on inclination angle for cases with $i \lesssim 40^o$, and the well known decrease in survival time at high ($i \gtrsim 40^o$) inclination angles. A simple extrapolation of our results for low inclination angles indicates that while potentially Hill unstable, orbital configurations with a companion mass of $M_C = 0.1 M_\odot$ and $M_C = 0.5 M_\odot$ can nonetheless remain stable for ~ 5 Gyrs when $p \gtrsim 4$ AU and $p \gtrsim 6$ AU, respectively. Note that these estimates are conservative in that the extrapolation is carried out along the lower envelope of the (wide) range of survival times for a given periastron. These results are consistent with those of D03, and represent lower periastron values than those obtained through a Hill stability analysis (e.g., Gladman 1993; see also Barnes & Greenberg 2006), i.e., systems that are ultimately "unstable" according to analytic criteria can survive over the 4.6 Gyr age of the Solar System.

This work has important implications for searches for Earth-like planets (e.g., Terrestrial Planet Finder) in extrasolar systems, since a large fraction of stars are found in binaries. As summarized above, our numerical results show that all binaries with periastron greater than 6–7 AU allow Earth-like planets to be stable over the age of our Solar System. This finding, in conjunction with the observed distributions of binary parameters for solar-type primaries (see Duquennoy & Mayor 1991 and the compilation of D03), indicates that roughly half of all binaries are wide enough to contain stable Earths. In addition, binaries that are wide enough (with sufficiently large periaston) to allow for orbital stability of Earth-like planets are also wide enough to allow for the formation of terrestrial planets through the accumulation of planetesimals (e.g., Quintana et al. 2002; Quintana 2004; Marzari & Scholl 2000). Thus, at least half of the binary systems are habitable according to dynamical considerations.

Some of the extrasolar planets detected to date are found in binary systems, although these planets have masses comparable to that of Jupiter. In the simulations performed here, the Earth-like planet acts like a test particle, but even a Jovian mass planet will act as a test particle in the potential of stellar bodies. As a result, one can directly apply our stability criteria to these systems: In order for a Jovian planet to remain stable over typical

stellar ages of ~ 5 Gyr, the binary periastron p_B must be wider than about ~ 7 times the semimajor axis a_J of the Jovian planet, i.e., $p_B \gtrsim 7a_J$. In all of the binary systems with detected planets, the periastron satisfies this constraint. A related question is whether or not an Earth-like planet can survive in a binary system that also contains a Jovian planet. Although the relevant 4-body simulations must be left for future work, a rough criterion can be formulated using our results to date: The Jovian planet must have a sufficently large periastron to allow the Eath-like planet to remain stable (and this constriant is roughly $p_J \gtrsim 2.5 - 3$ AU, e.g., D03) and the binary periastron p_B must be large enough to allow the Jovian planet to be stable (roughly $p_B \gtrsim 7p_J$).

The next major result of this work concerns the width of the distributions of survival time. We have calculated the μ_s distributions over a broad range of orbital parameter space. It is well known that orbital systems can exhibit chaotic behavior in or near the unstable regime. As a result, it is not possible to define a unique value of survival time for a given orbital configuration. Instead, the survival time can only be defined in terms of a distribution – the mean and width of which then characterizes the underlying dynamics of the system. For the orbital configurations explored in series 1 – 4, the resulting μ_s distributions exhibit Gaussian peaks with widths $\sigma \sim 0.5$ and generally display high-end tails when $\langle \mu_s \rangle \gtrsim 4$. In this regime, the value of $\langle \mu_s \rangle$ calculated via N equivalent realizations of a given orbital configuration has a 68% probability of being within $0.05\sqrt{(100/N)}$ of the true value, and a 99% probability of being within $0.15\sqrt{(100/N)}$ of the true value. The situation is more complex for orbital configurations whose μ_s distributions have means in excess of ~ 4. While exhibiting peaks with widths ~ 0.5, these distributions may also have significant tails, thereby leading to larger calculated total width values ($\sim 0.7 - 2$). Part of this increased complexity can be traced to the increasing importance of mean motion orbital resonance effects. Additionally, the loss of a tangential component in the impulse imparted as the planet moves through closest approach for low eccentricity cases can also lead to fairly broad distributions, although the paucity of observed low eccentricity binary systems somewhat limits the importance of this latter effect. Nevertheless, our results indicate that the determination of survival times for long-lived systems poses a serious numerical challenge in that both the integration times must be longer and (because of the broader distributions) a larger number of equivalent realizations must be performed in order to get good statistical results.

The form of the distributions of survival times is not unexpected. Whenever a large number of independent variables play a role in determining a distribution, the result tends to exhibit a nearly gaussian form. In the limit of an infinite number of variables, the central limit theorem indicates that the resulting distribution will be gaussian, for any type of distribution for the input variables (e.g., Richtmyer 1978). Binary systems with planets contain an

intermediate number of variables. Although the systems are sufficiently complicated to display interesting and complex behavior (Figs. 1 – 18), the number of independent variables in not infinite. As a result, one expects the distribution of any composite variable (here the survival time for a given orbital configuration) to approach a gaussian form, but retain non-gaussian tails (since convergence is slowest in the tails). The result – a gaussian distribution with tails – is in fact what we find here.

As expected from the chaotic nature of the systems being explored, our output measures exhibit a rich amount of structure. Specifically, we find that the presence of Kozai resonances result in a region of stability at $i \sim 60^o$ when the companion orbit has a low eccentricity. In addition, we find a significant amount of structure in the output measure f_e - the fraction of events that lead to ejection for a given orbital configuration. To our knowledge, this latter result has not received significant attention in the literature, and may warrant further study.

Acknowledgments

We thank Matt Holman for useful discussions. This work was supported at Xavier University by the Hauck Foundation, and by the National Science Foundation under Grant No. 0215836. This work was supported at the University of Michigan by the Michigan Center for Theoretical Physics, and by NASA through the Terrestrial Planet Finder Mission (NNG04G190G) and the Astrophysics Theory Program (NNG04GK56G0). Finally, we thank the referee for a comprehensive set of comments that improved the manuscript.

REFERENCES

Asghari, N., Broeg, C., Carone, L., et al. 2004, A&A, 426, 353

Barnes, R., & Greenberg, R. 2006, ApJ Lett, in press

Butler, R. P., et al. 1999, ApJ, 526, 916

David, E.-M., Quintana, E. V., Fatuzzo, M., & Adams, F. C. 2003, PASP, 115, 825 (D03)

Duquennoy, A., & Mayor, M. 1991, A&A, 248, 485.

Dvorak, R., Froeschle, C., & Froeschle, Ch. 1989, A&A, 226, 335

Eggenberger, A., Udry, S., & Mayor, M. 2004, A&A, 417, 353

Fischer, D. A., et al. 2002, ApJ, 564, 1028

Gladman, B. 1993, Icarus, 106, 247

Haghighipour, N. 2006, ApJ, 644, 543

Harrington, R. S. 1977, AJ, 82, 753

Holman, M. J., & Wiegert, P. A. 1999, AJ, 117, 621

Innanen, K. A., Zheng, J. Q., Mikkola, S., & Valtonen, M. J. 1997, AJ, 113, 1915

Jones, B. W., Underwood, D. R., & Sleep, P. N. 2005, ApJ, 622, 1091

Kozai, Y. 1962, AJ, 67, 591.

Laughlin, G., & Adams, F. C. 1999, ApJ, 526, 881

Lissauer, J. J. 1993, ARA&A, 31, 129

Lissauer, J. J., Quintana, E. V., Chamnbers, J. E., Duncan, M. J., & Adams, F. C. 2004, RevMexAA (Series de Conferencias), 22, 99

Marcy, G. W., Butler, R. P., Vogt, S. S., et al. 2001, ApJ, 555, 418

Marzari, F., & Scholl, H. 2000, ApJ, 543, 328

Mathieu, R. D., Adams, F. C., & Latham, D. W. 1991, AJ, 101, 2184

McArthur, B. E., Endl, M., Cochran, W. D., et al. 2004, ApJ, 614, L81

Mudryk, L. R., & Wu, Y. 2006, ApJ, 639, 423

Murray, C. D., & Dermott, S. F. 2000, Solar System Dynamics (Cambridge: Cambridge Univ. Press)

Musielak, Z. E., Cuntz, M., Marshall, E. A., & Stuit, T. D. 2005, A&A 434, 355

Noble, M., Musielak, Z. E., & Cuntz, M. 2002, ApJ, 572, 1024

Pendleton, Y. J., & Black, D. C. 1983, AJ, 88, 1415

Pilat-Lohinger, E. & Dvorak, R. 2002, CeMDA, 82, 143

Pilat-Lohinger, E., Funk, B., & Dvorak, R. 2003, A&A, 400, 1085

Press, W. H., et al. 1992, Numerical Recipes: The art of scientific computing (Cambridge: Cambridge Univ. Press)

Quintana, E. V., Lissauer, J. J., Chambers, J. E., & Duncan, M. J. 2002, ApJ, 576, 982

Quintana, E. V. 2004, PhD Thesis, University of Michigan

Rabl, G., & Dvorak, R. 1988, A&A, 191, 385

Richtmyer, R. D. 1978, Principles of Advanced Mathematical Physics (New York: Springer-Verlag)

Ruden, S. P. 1999, in Origin of Stars and Planetary Systems, ed. C. J. Lada & N. D. Kylafis (Dordrech: Kluwer), 643

Süli, Á, Dvorak, R., & Florian, F. 2005, MNRAS, 363, 241

Szebehely, V. 1967, Theory of orbits: The restricted problem of three bodies (New York: Academic Press)

Tinney, C. G., et al. 2002, ApJ, 571, 528

Whitmire, D. P., Matese, J. J., Criswell, L., & Mikkola, S. 1998, Icarus, 132, 196

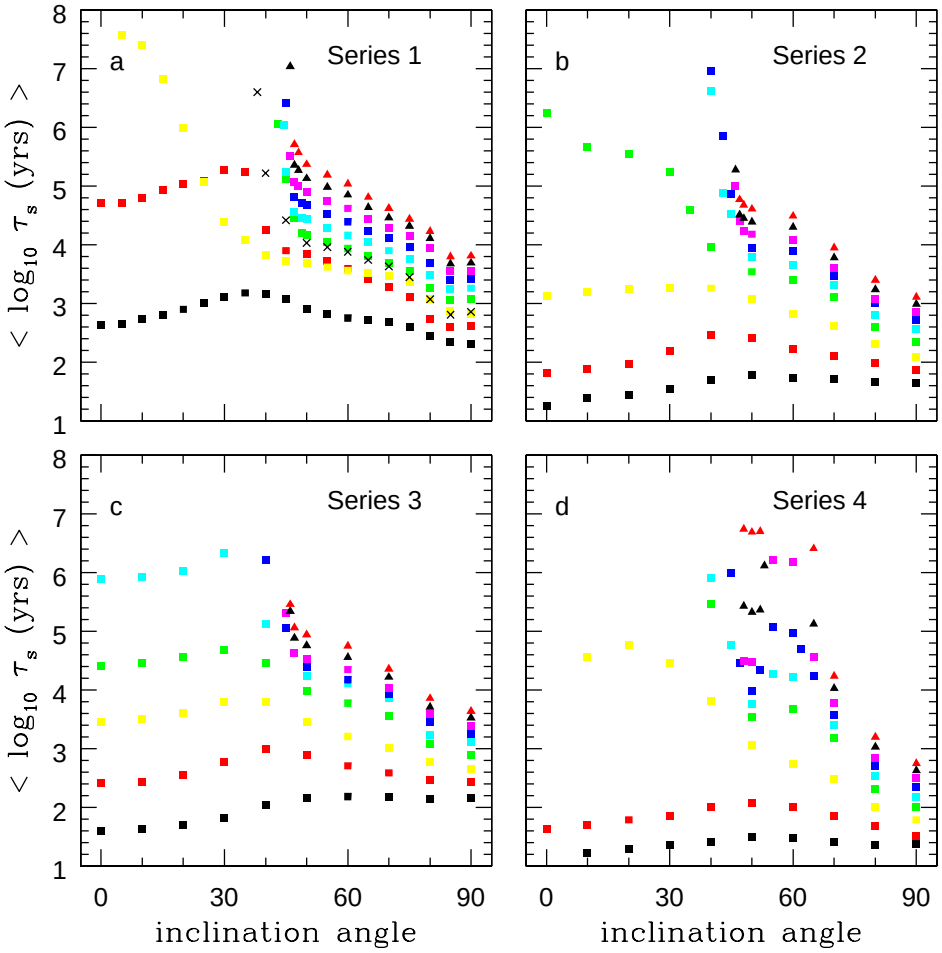

Fig. 1.— Results of numerical simulations for each of the series 1 – 4, as labeled in each panel. The mean of the $\mu_s = \log \tau_s$ distribution generated for each orbital configuration is plotted versus inclination angle (degrees) for periastron values (in AU) of: 2 (black squares); 2.5 (red squares); 2.9 (×); 3 (yellow squares); 3.5 (green squares); 4 (light blue squares); 4.5 (dark blue squares); 5 (purple squares); 5.5 (black triangles); and 6 (red triangles).

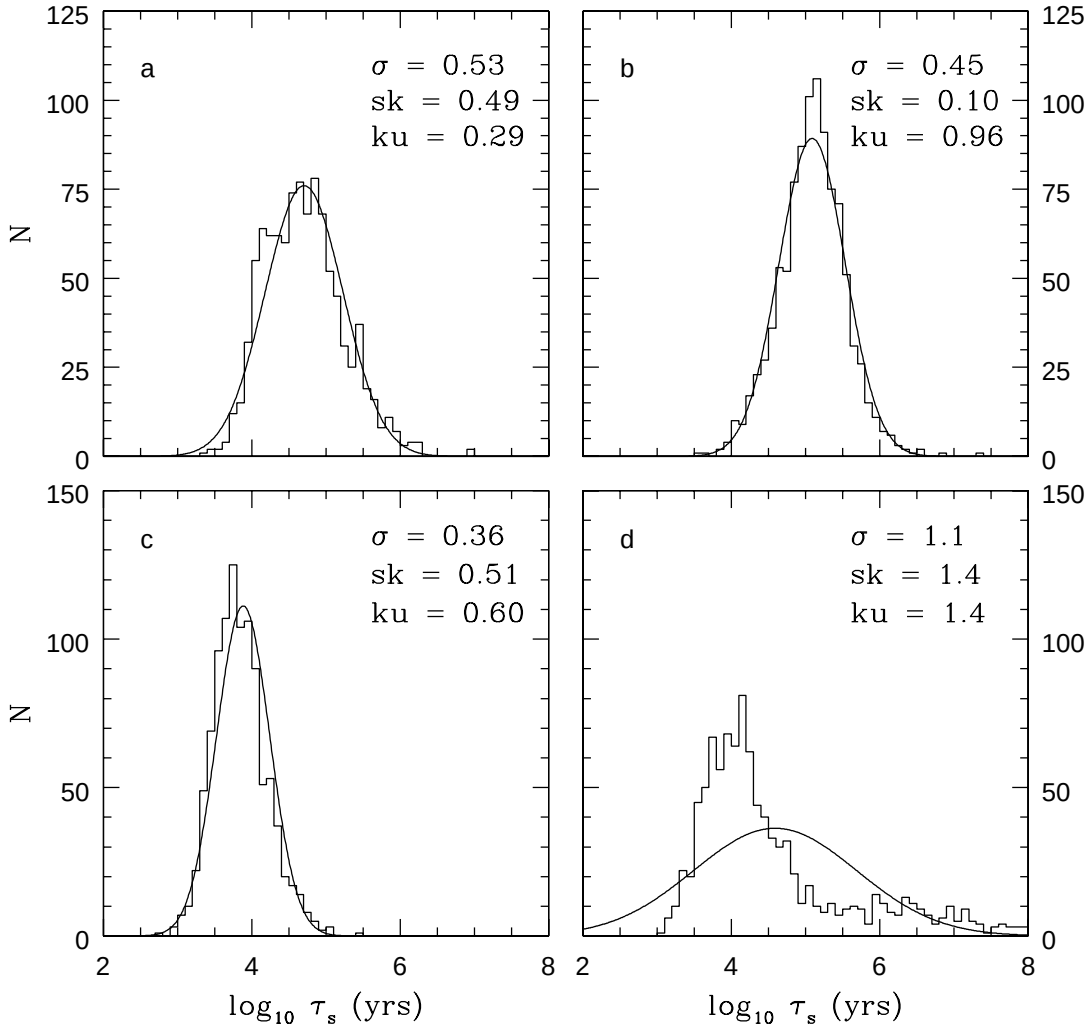

Fig. 2.— The distributions of $N = 10^3$ equivalent values of $\mu_s = \log \tau_s$ (i.e., set through a random sampling of the initial phase angles) for the following four orbital configurations: Panel (a) – $M_C = 0.1 M_\odot$, $p = 2.5$ AU, $e = 0.5$, and $i = 0^o$; Panel (b) – same as panel (a), but with $i = 25^o$; Panel (c) – same as panel (a), but with $i = 50^o$; Panel (d) – $M_C = 0.5 M_\odot$, $p = 3.5$ AU, $e = 0.5$, and $i = 35^o$. The calculated distribution width, skew and kurtosis for each distribution is shown in each panel. The solid curve shows a normal distribution with the same mean and width as the computed distributions, normalized to the sample size of $N = 10^3$.

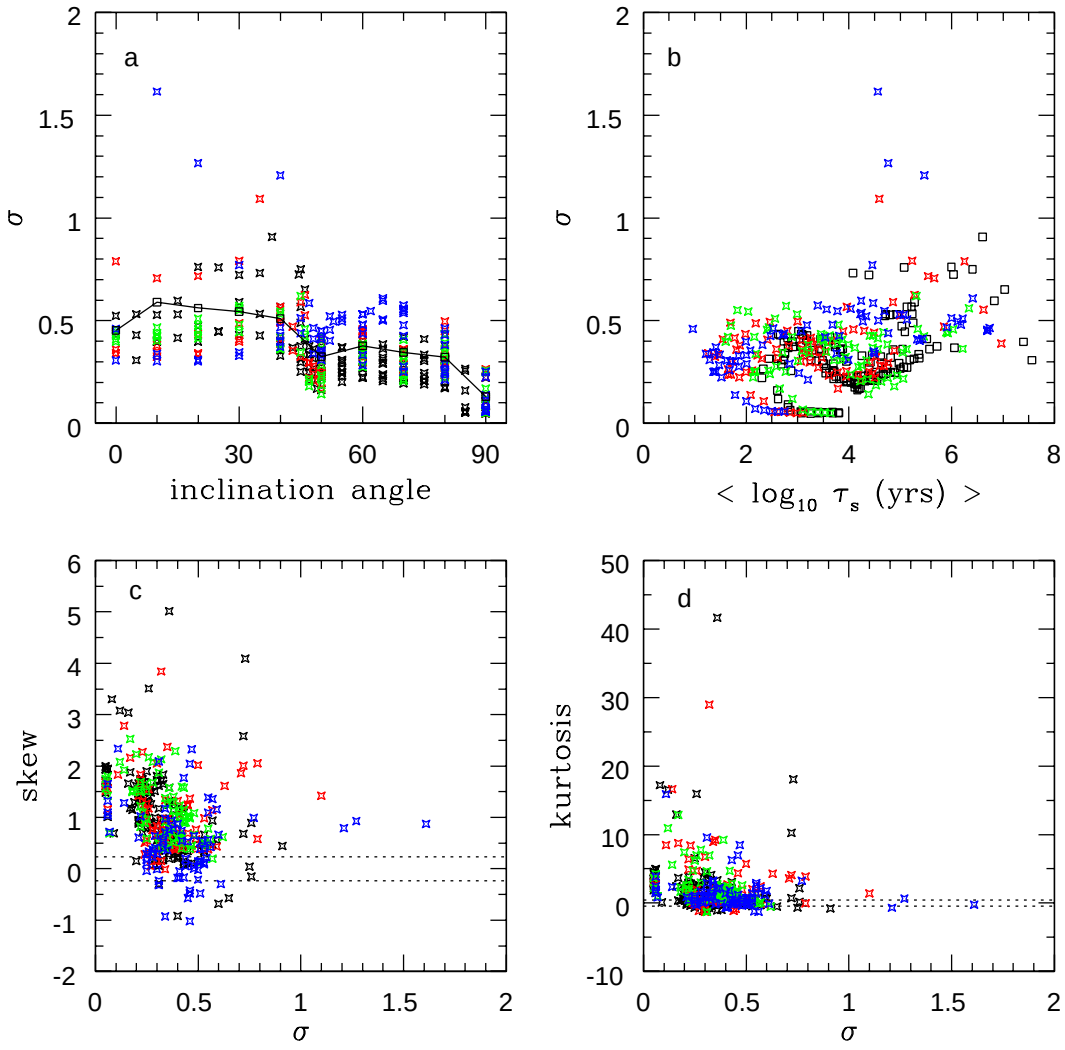

Fig. 3.— Scatter plots of the output measures derived from the μ_s distributions of the orbital configurations in series 1 – 4. Panel (a) – width versus inclination angle; Panel (b) – width versus mean; Panel (c) – skew versus width; Panel (d) – kurtosis versus width. Results from each series in all four panels are denoted using the following color scheme: series 1 – black; series 2 – red; series 3 – green; series 4 – blue. The solid line in panel (a) connects the mean widths calculated at each inclination angle, determined by combining all of the results from orbital configurations with the same inclination angle (but offset by the mean so as to center each distribution about zero) to form a single distribution, and then calculating the ensuing width as per equation (1). The dotted lines in panels (c) and (d) represent the three sigma values for the skew and kurtosis distributions, respectively, generated by randomly sampling a normal parent distribution $N = 10^3$ times.

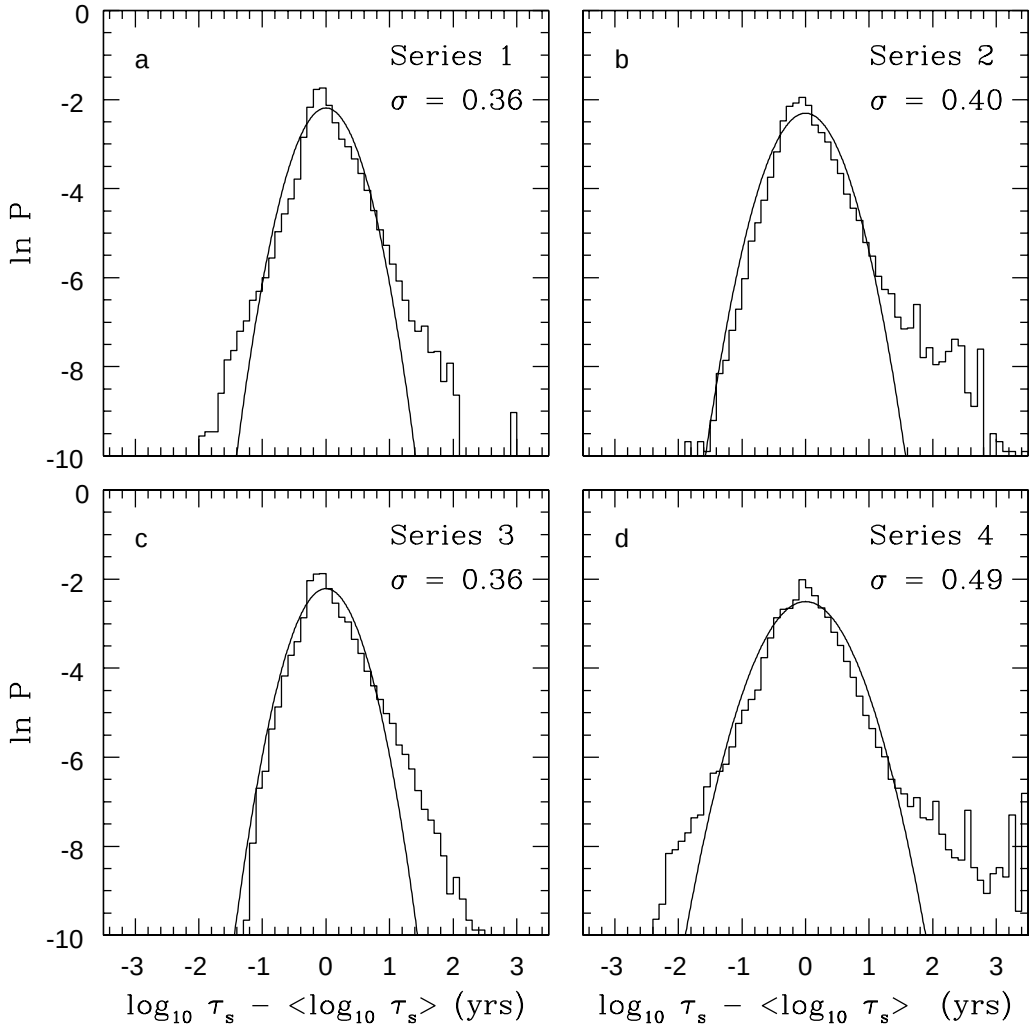

Fig. 4.— The distribution of all of the survival times for orbital configurations in: Panel (a) – series 1; Panel (b) – series 2; Panel (c) – series 3; and Panel (d) – series 4. Each value of μ_s has been offset by the mean value of its orbital configuration distribution to ensure proper normalization. Distributions are plotted in terms of the natural log of the probability of being in a specified bin. The solid curve in each panel shows a normal distribution with the same width as the computed distributions, normalized to unity.

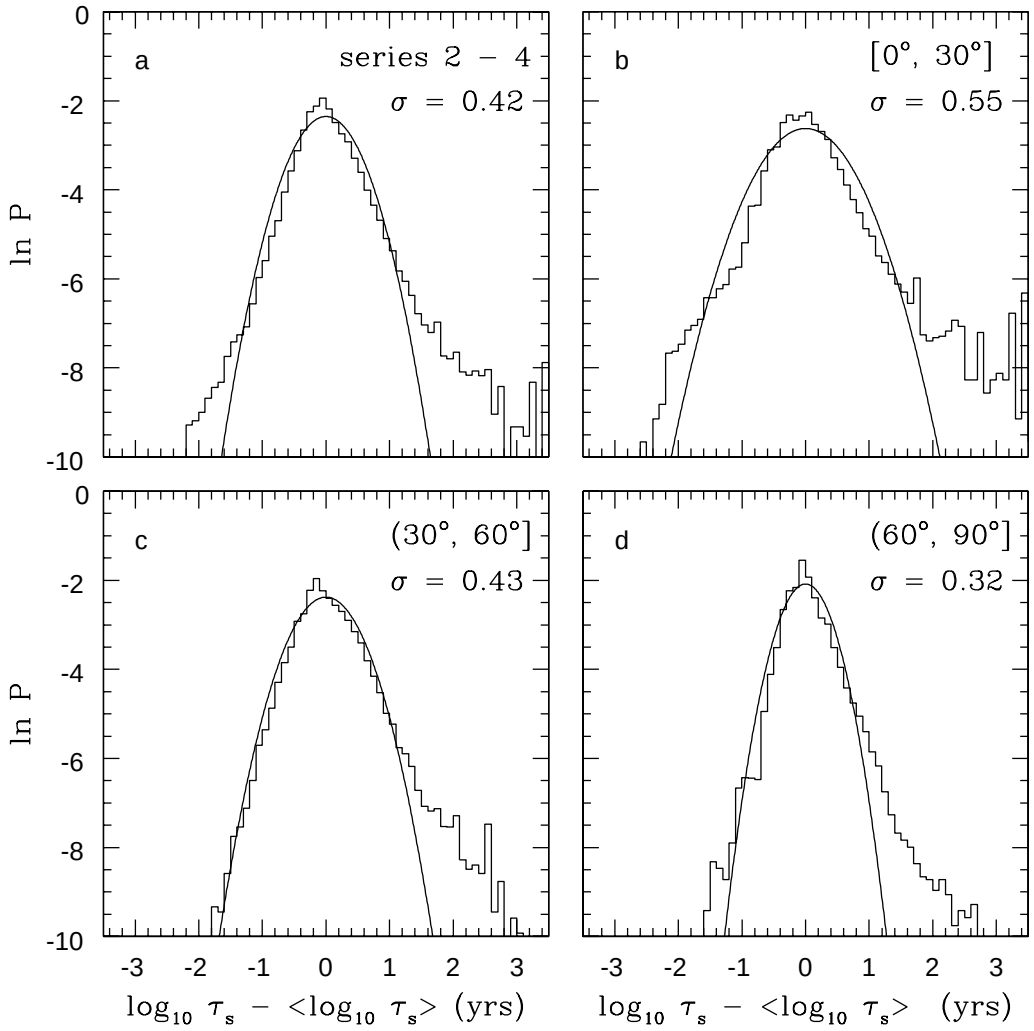

Fig. 5.— Same as Fig. 4, but for: Panel (a) – all orbital configurations in series 2 – 4; Panel (b) – the subset of series 2 - 4 orbital configurations with inclination angles $0^o \leq i \leq 30^o$; Panel (c) – same as panel (b), but for $30^o < i \leq 60^o$; Panel (d) – same as panel (b), but for $60^o < i \leq 90^o$.

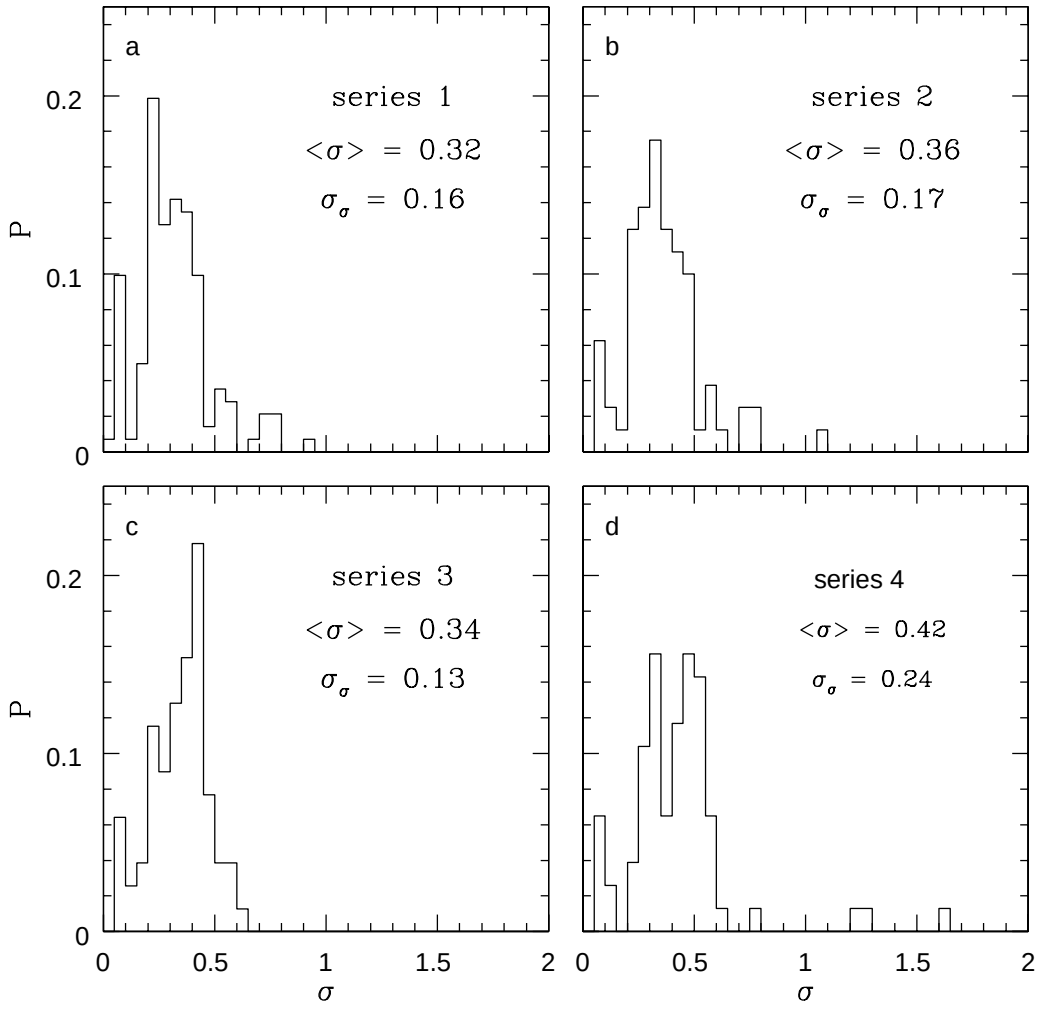

Fig. 6.— The distribution of widths calculated from the μ_s distributions for the orbital configurations in: Panel (a) – series 1; Panel (b) – series 2; Panel (c) – series 3; Panel (d) – series 4. The calculated mean $\langle\sigma\rangle$ and width σ_σ of the distributions shown in each panel are also presented.

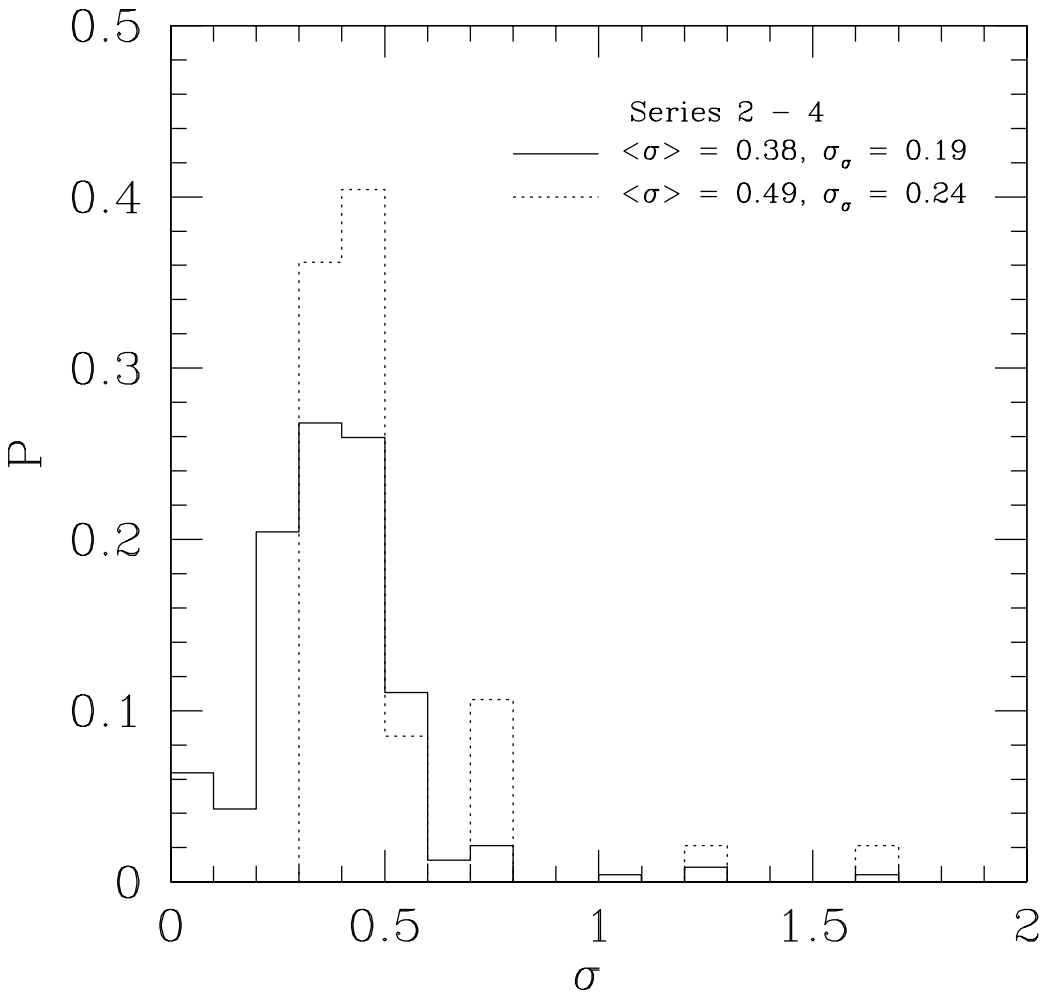

Fig. 7.— Same as Fig. 6, but for all of the orbital configurations in series 2 – 4 (solid line) as well as for the $0^o \leq i \leq 30^o$ subset (dotted line).

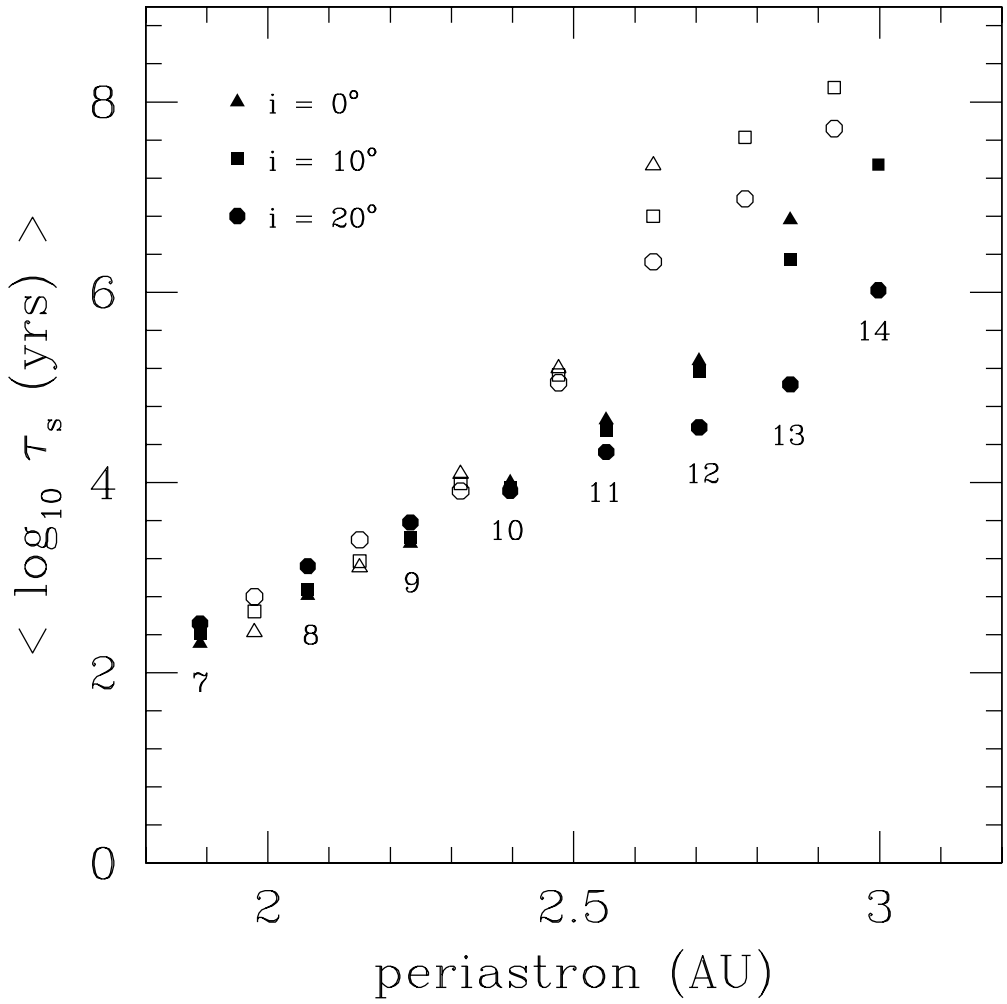

Fig. 8.— Results of numerical simulations for series 5 ($M_C = 0.1 M_\odot$ and $e = 0.5$). The mean of the μ_s distribution generated for each orbital configuration is plotted versus periastron for the following inclination angles: 0^o – triangles; 10^o – squares; 20^o – circles. Values from $n_C : 1$ orbital configurations are represented with solid points, and the value of n_C is marked below the corresponding data. Values from $n_C : 2$ orbital configurations are represented by open points, with the value of n_C implied by their location.

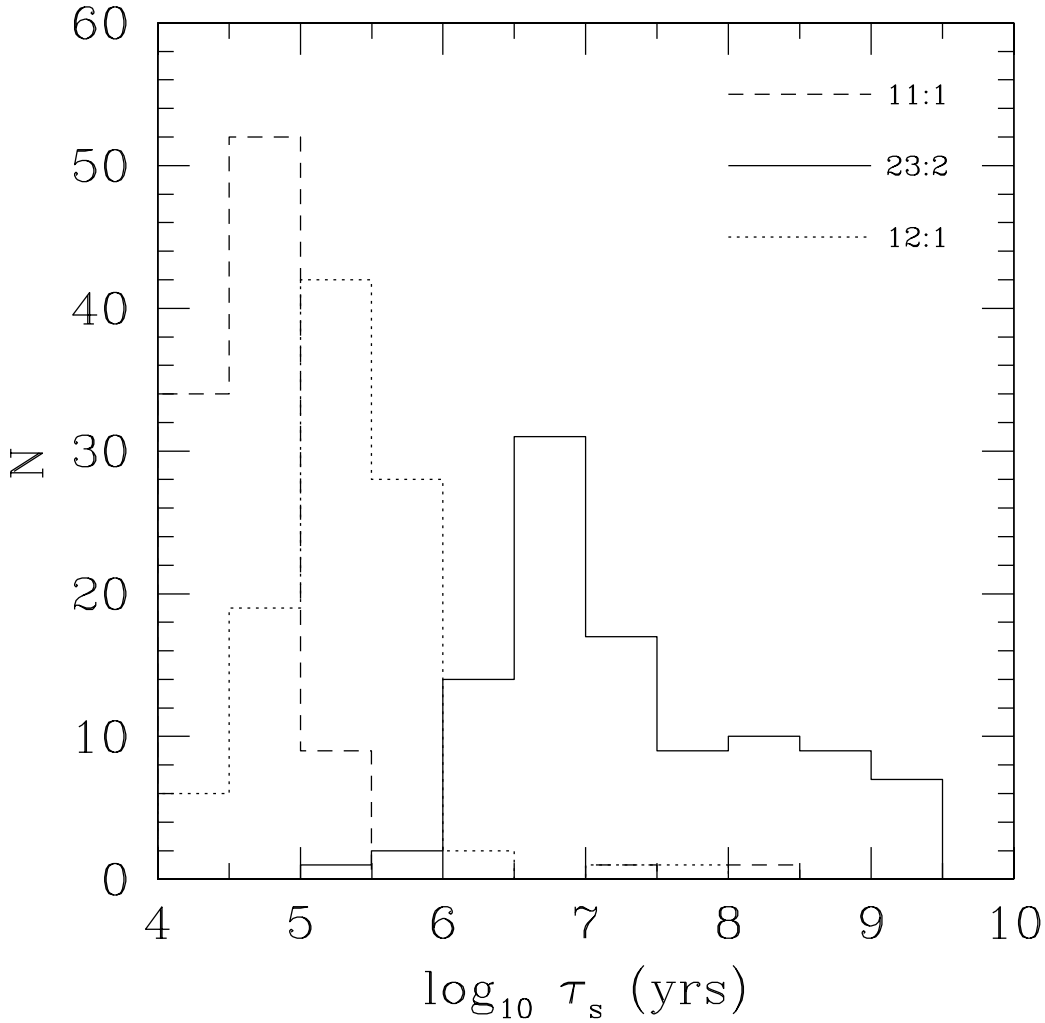

Fig. 9.— The distribution of μ_s values for three orbital configuration from series 5. Long dashed line – $p = 2.553$ AU ($n_C : n_p = 11 : 1$); Solid line – $p = 2.630$ AU ($n_C : n_p = 23 : 2$); Dotted line – $p = 2.705$ AU ($n_C : n_p = 12 : 1$).

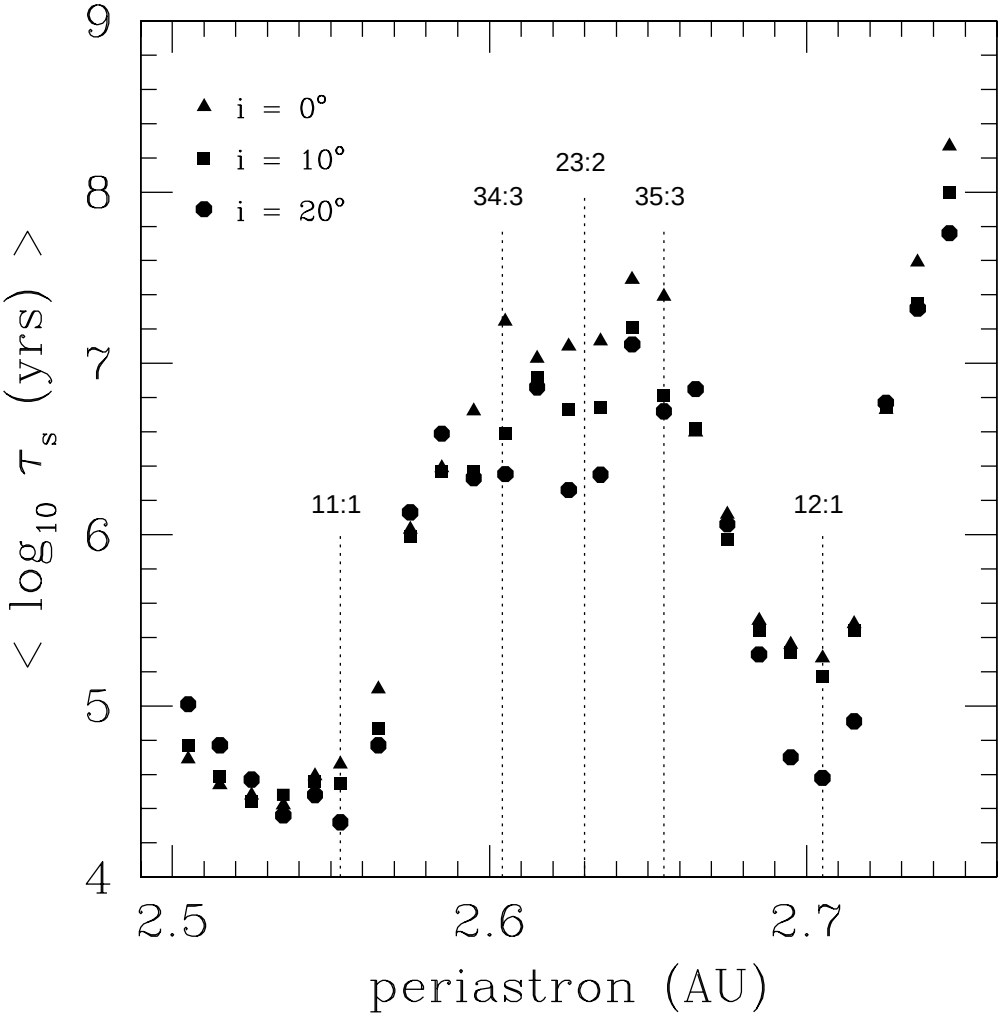

Fig. 10.— Same as Fig. 8, but for a narrower range of periastron values. Vertical dotted lines denote periastron values for which integer ratios of initial orbital periods occur, with the corresponding $n_C : n_p$ values labeled above.

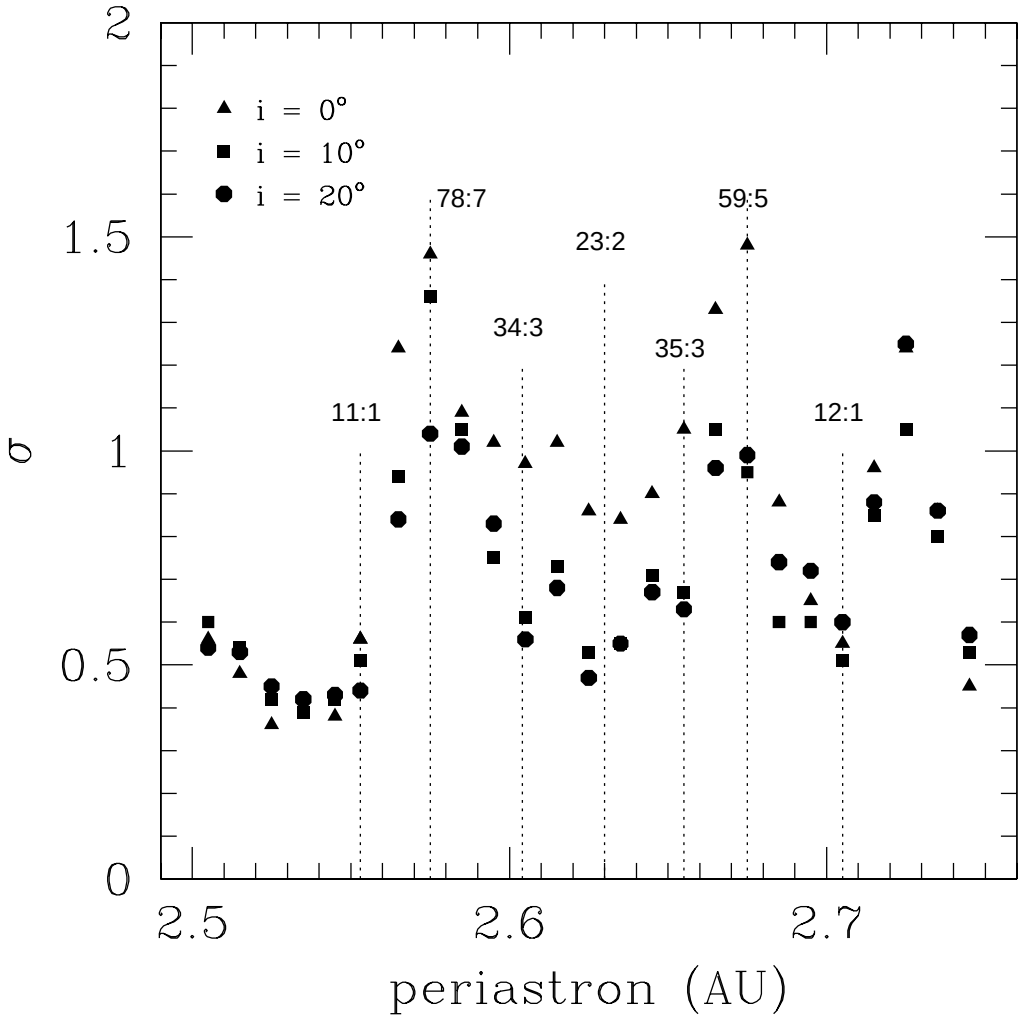

Fig. 11.— The width of the distributions for the orbital configurations in series 6 as a function of periastron for the following inclination angles: 0^o – triangles; 10^o – squares; 20^o – circles. Vertical dotted lines denote periastron values for which integer ratios of initial orbital periods occur, with the corresponding $n_C : n_p$ values labeled above.

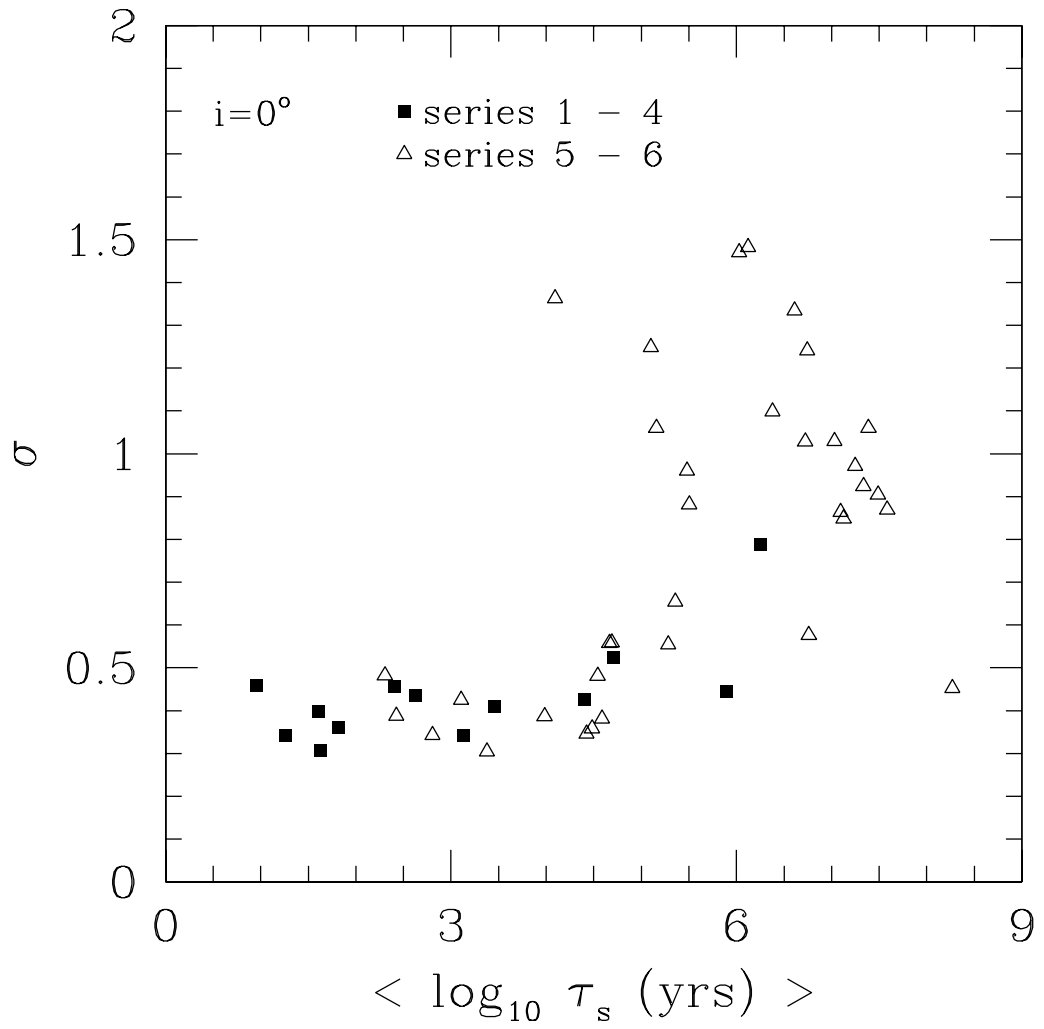

Fig. 12.— The scatter plot of width versus mean for the distributions of the $i = 0^o$ orbital configurations in series 1 – 4 (solid squares) and series 5 – 6 (open triangles).

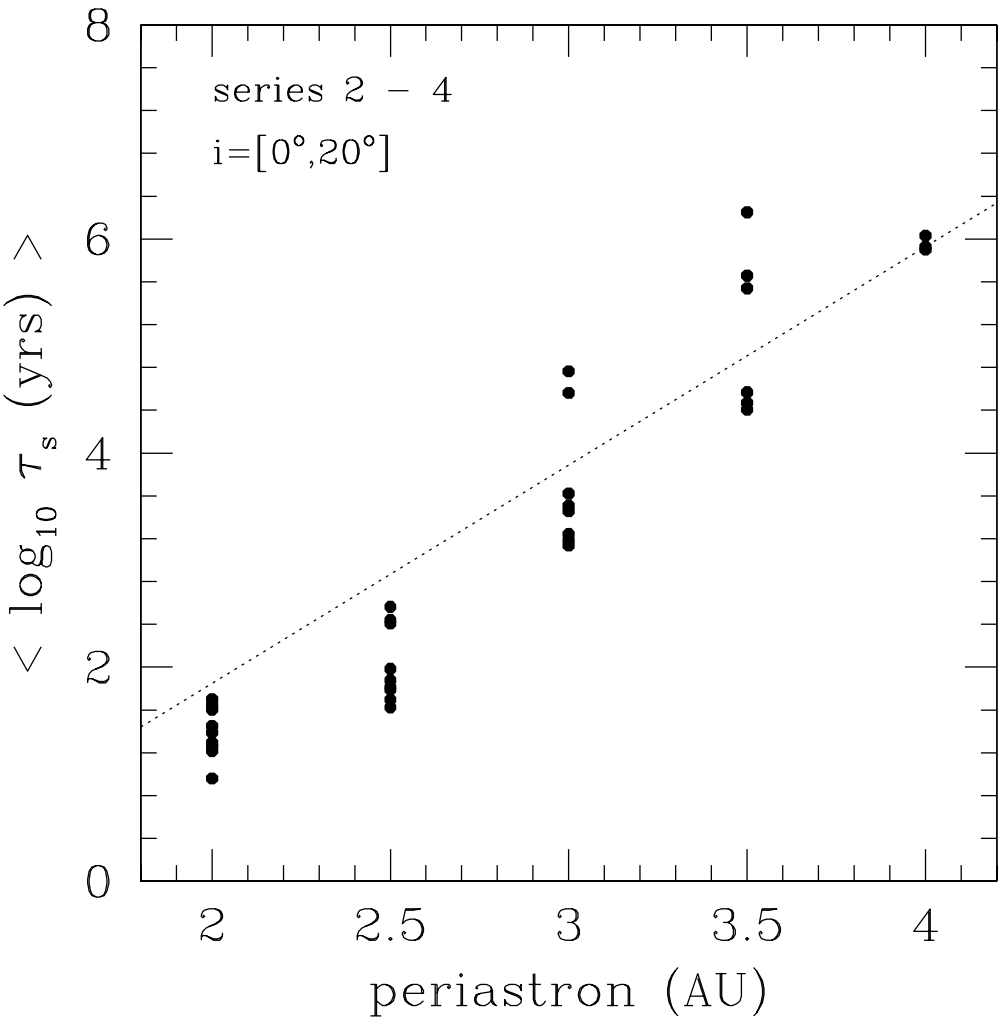

Fig. 13.— Results of numerical simulations for series 2 – 4 ($M_C = 0.5 M_\odot$). The mean of the normal distribution generated for each orbital configuration is plotted versus periastron for inclination angles $0^o \leq i \leq 20^o$. The dotted line plots the ejection time given by equation (4) with values of $\alpha = 4.7$ and $\tau_{s0} = 0.64$ (the best fit values to the corresponding data presented in D03, Figure 3).

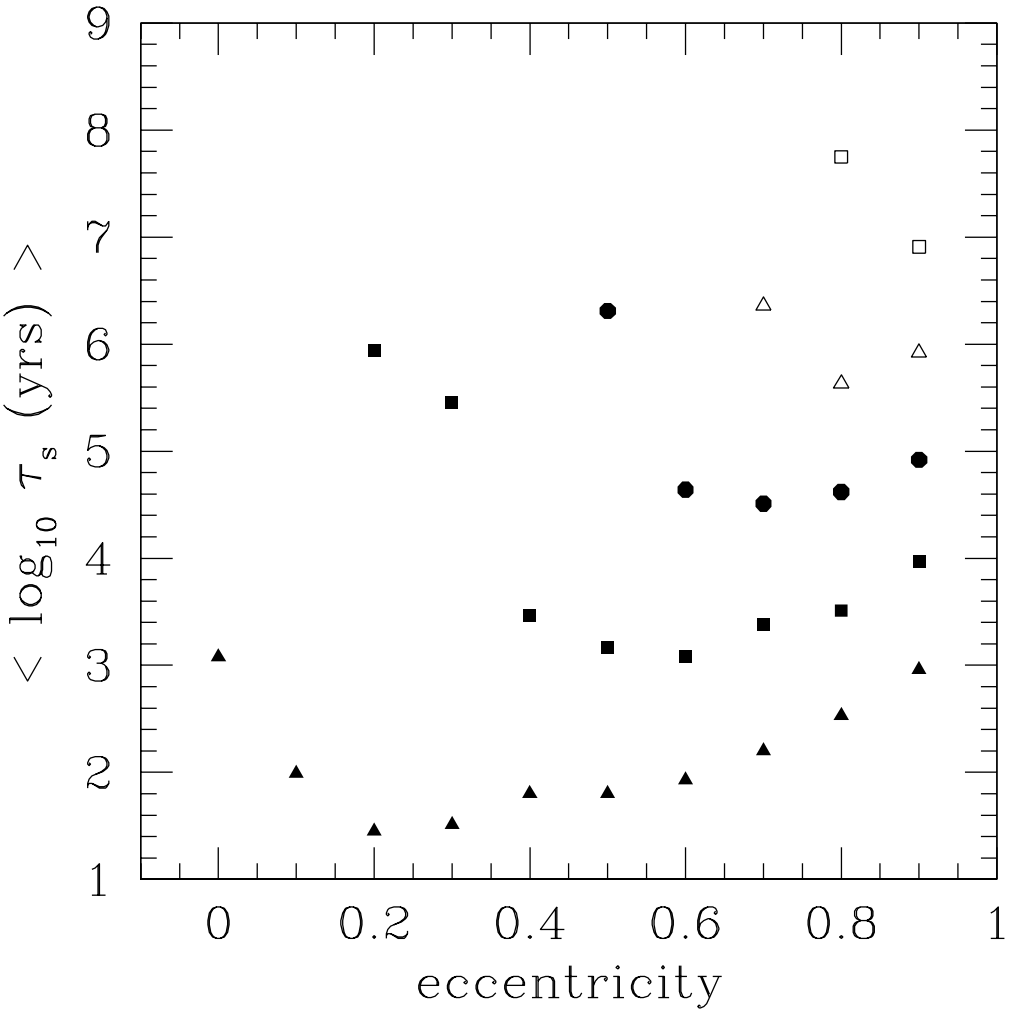

Fig. 14.— Results of numerical simulations for series 7 ($M_C = 0.5 M_\odot$ and $i = 0^o$). The mean of the μ_s distributions generated for each orbital configuration is plotted versus companion eccentricity for periastron values (in AU): 2.5 (solid triangles); 3 (solid squares); 3.5 (solid circles); 4 (open triangles); and 4.5 (open squares).

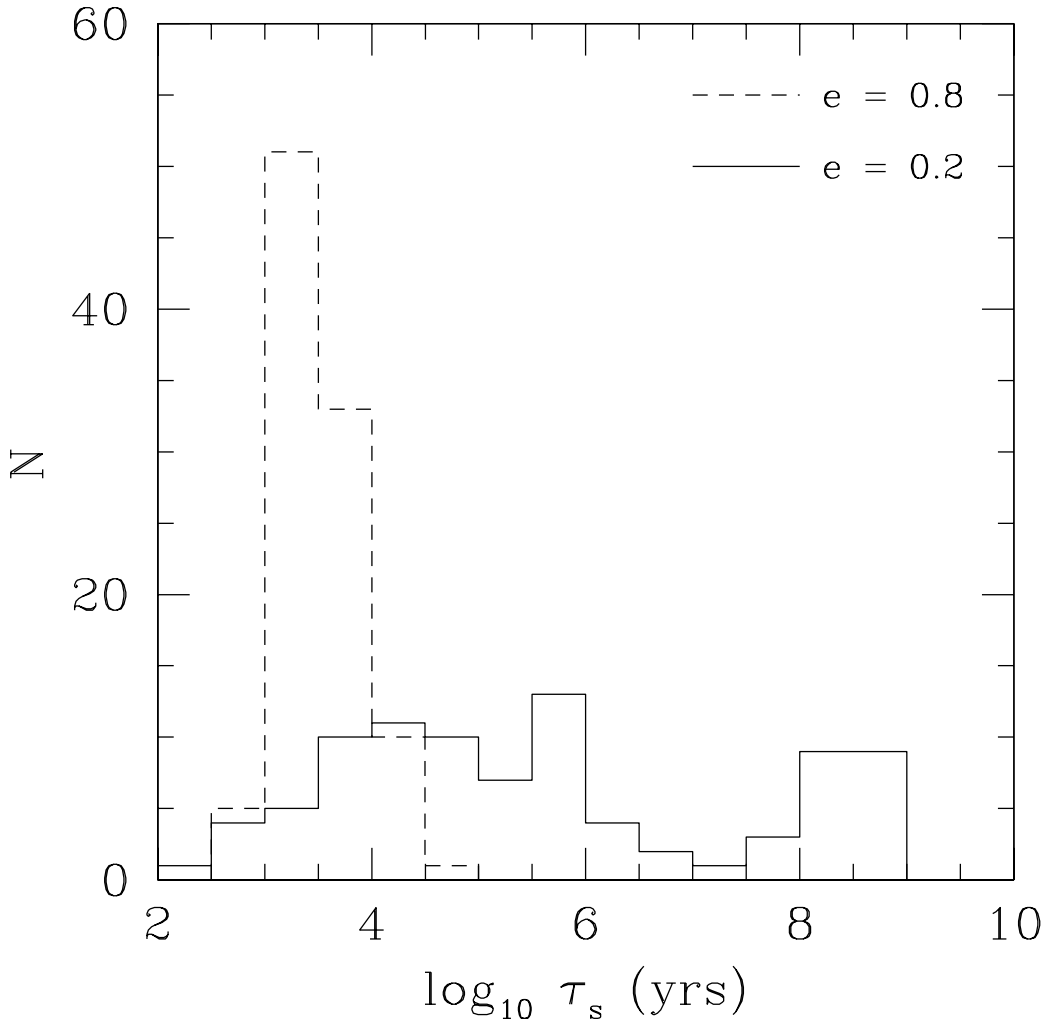

Fig. 15.— The distributions of survival times for two orbital configurations from series 7, with $M_C = 0.5 M_\odot$, $p = 3$ AU, $i = 0^o$ and $e = 0.2$ (solid line) and $e = 0.8$ (dotted line).

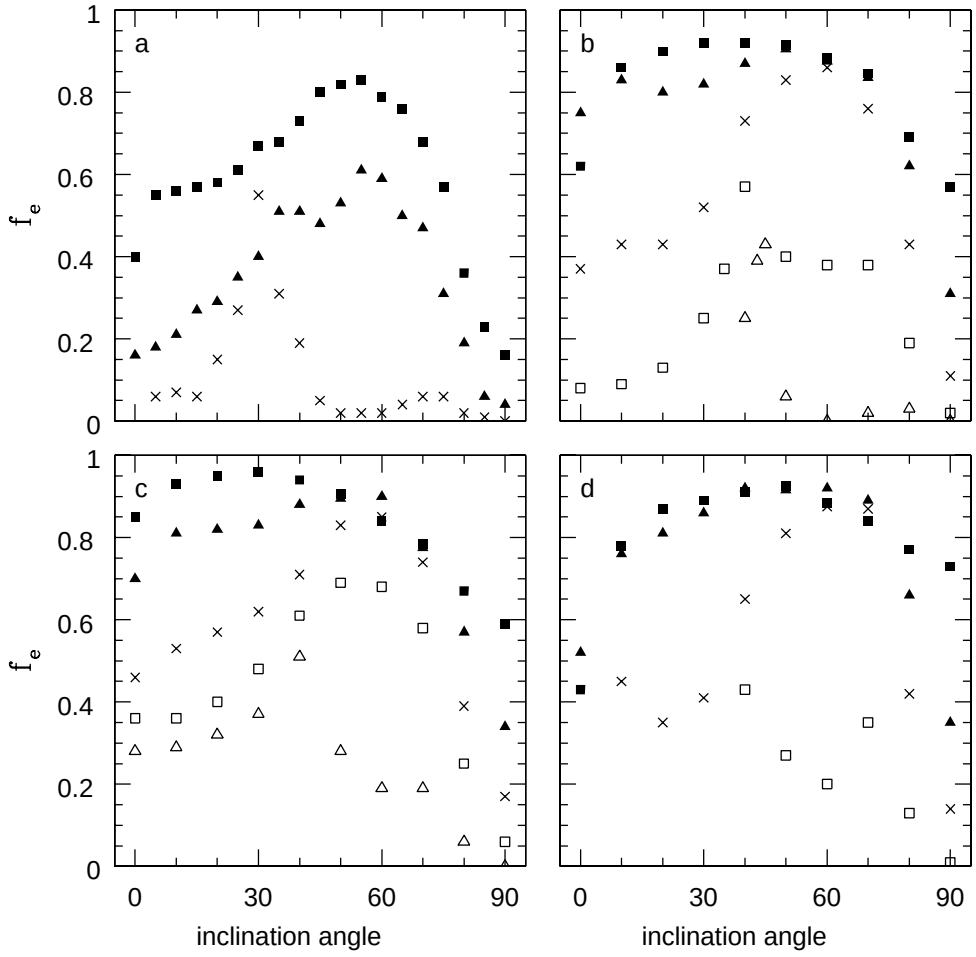

Fig. 16.— The fraction of all simulations (excluding those which survive out to the integration time τ_{run}) leading to ejection is plotted versus inclination angle for periastron values (in AU): 2 (solid square); 2.5 (solid triangle); 3 (×); 3.5 (open square); 4 (open triangle). Panel (a) – series 1; Panel (b) – series 2; Panel (c) – series 3; and Panel (d) – series 4.

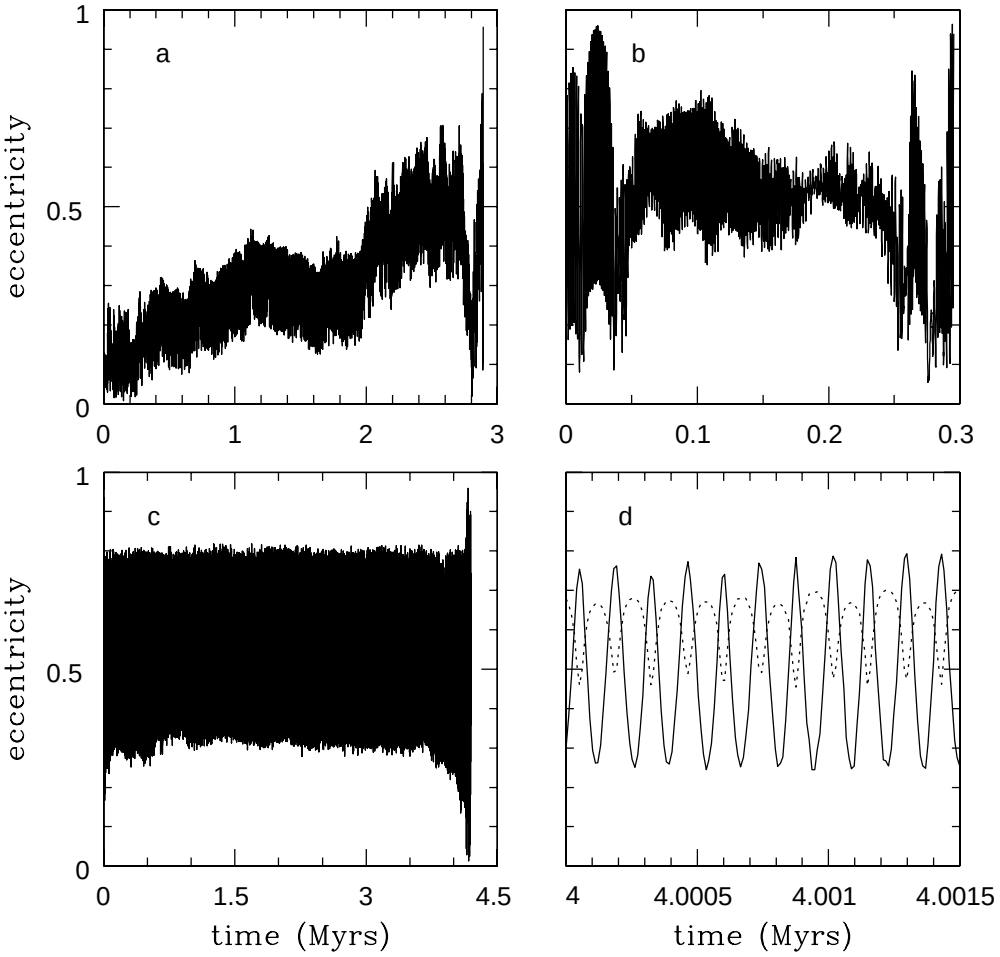

Fig. 17.— The time evolution of the planet's eccentricity for three numerical experiments with different orbital configurations. Panel (a) – Run 1: $M_C = 0.5 M_\odot$, $p = 4$ AU, $e = 0.75$ and $i = 0^o$; Panel (b) – Run 2: $M_C = 0.5 M_\odot$, $p = 4$ AU, $e = 0.75$ and $i = 60^o$; Panel (c) – Run 3: $M_C = 0.5 M_\odot$, $p = 4$ AU, $e = 0.25$ and $i = 60^o$; Panel (d) – same as panel (c), but for a small time interval of the planet's evolution. This panel also shows the planet's inclination angle (dotted line), as a fraction of $\pi/2$.

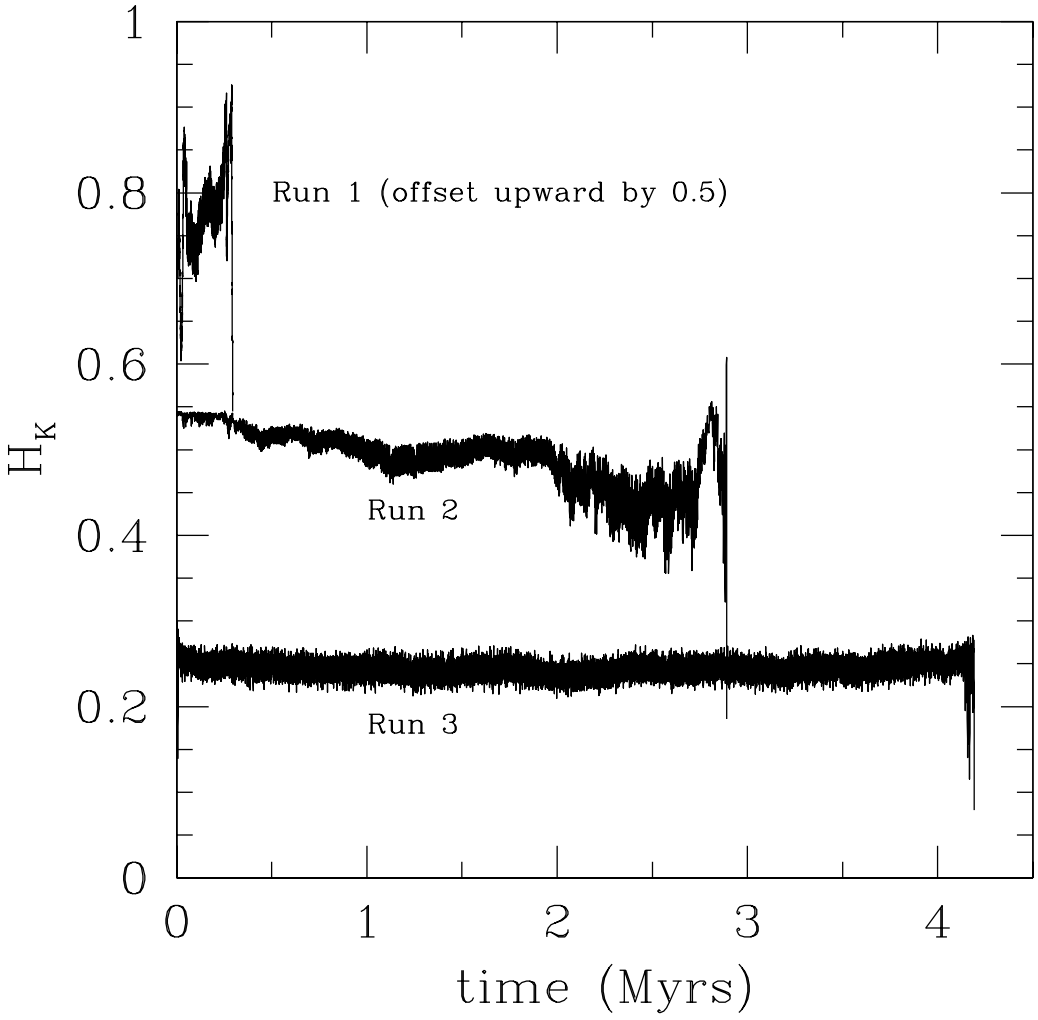

Fig. 18.— The time evolution of $H_K = \sqrt{a_C(1-e^2)}\cos i$ for the three numerical experiments presented in Figure 17. The value for Run 1 is offset upward by 0.5.